Nuclear Physics Aspects of Coherent Elastic Neutrino-Nucleus Scattering (CEvNS)

Vishvas Pandey

with N. Van Dessel, N. Jachowicz, H. Ray

arXiv:2007.03658 [nucl-th]

Fermilab | UF UNIVERSITY of FLORIDA | U.S. DEPARTMENT OF ENERGY | Office of Science

Outline

- Stopped pion sources and CEvNS
- CEvNS formalism: cross section and form factors
- Nuclear model: HF-SkE2
- Constraining ^{40}Ar
  - Weak form factor and CEvNS cross section
  - Inelastic cross section

Outline

- **Stopped pion sources and CEvNS**
- CEvNS formalism: cross section and form factors
- Nuclear model: HF-SkE2
- Constraining ^{40}Ar
  - Weak form factor and CEvNS cross section
  - Inelastic cross section

Stopped pion sources and CEvNS

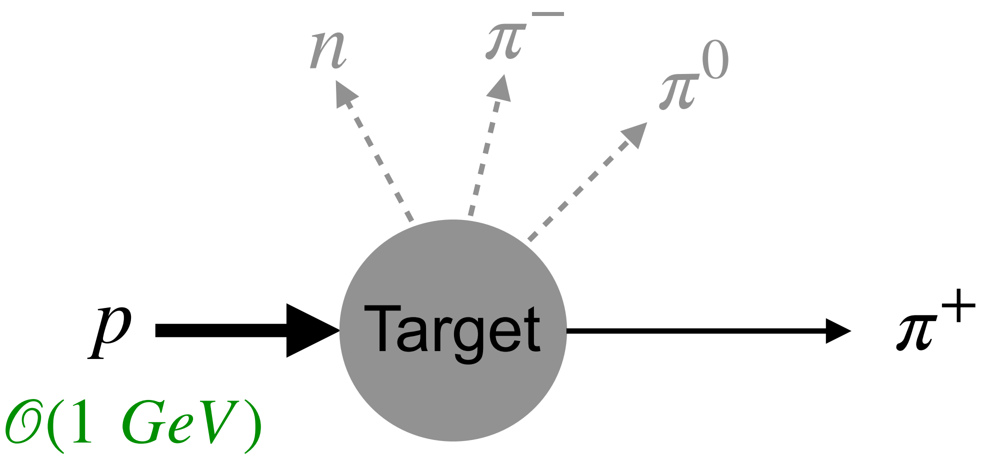

- **<u>Proton energy</u>:**

  - Sufficient energy (~1 GeV) to produce pions
    [SNS at ORNL, Lujan at LANL]

  - Higher energies lead to heavier mesons: kaons (> 3GeV), eta
    [JPARC-MLF]

- **<u>Target</u>:**

  - Heavier targets at spallation sources massively produce neutrons (primary motive)
    [Hg at SNS at ORNL and JPARC-MLF, W at Lujan at LANL]

  - Lighter targets preferred, low neutrons from beam

  - Neutrons mimic the same signature as CEvNS

Stopped pion sources and CEvNS

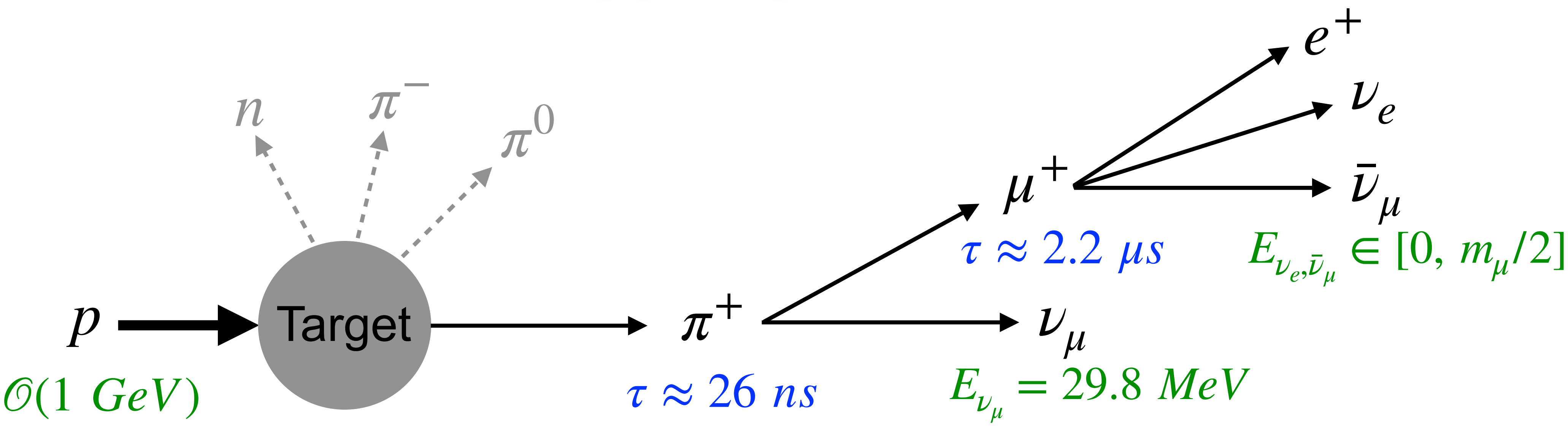

- **Proton energy**:

  - Sufficient energy (~1 GeV) to produce pions
    [SNS at ORNL, Lujan at LANL]

  - Higher energies lead to heavier mesons: kaons (> 3GeV), eta
    [JPARC-MLF]

- **Target**:

  - Heavier targets at spallation sources massively produce neutrons (primary motive)
    [Hg at SNS at ORNL and JPARC-MLF, W at Lujan at LANL]

  - Lighter targets preferred, low neutrons from beam

  - Neutrons mimic the same signature as CEvNS

Stopped pion sources and CEvNS

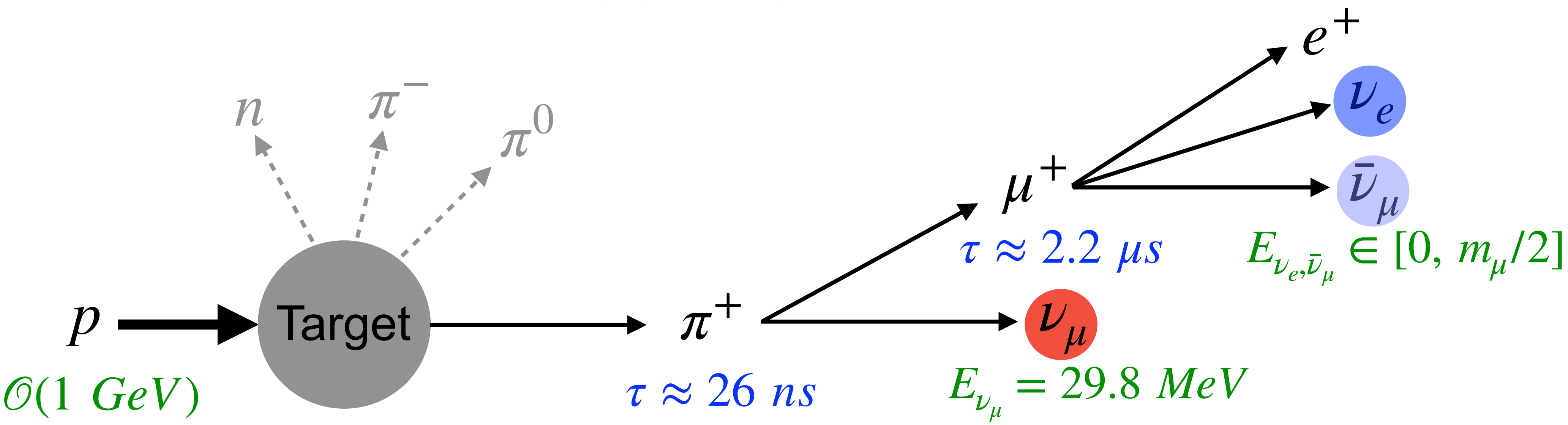

Timing Profile

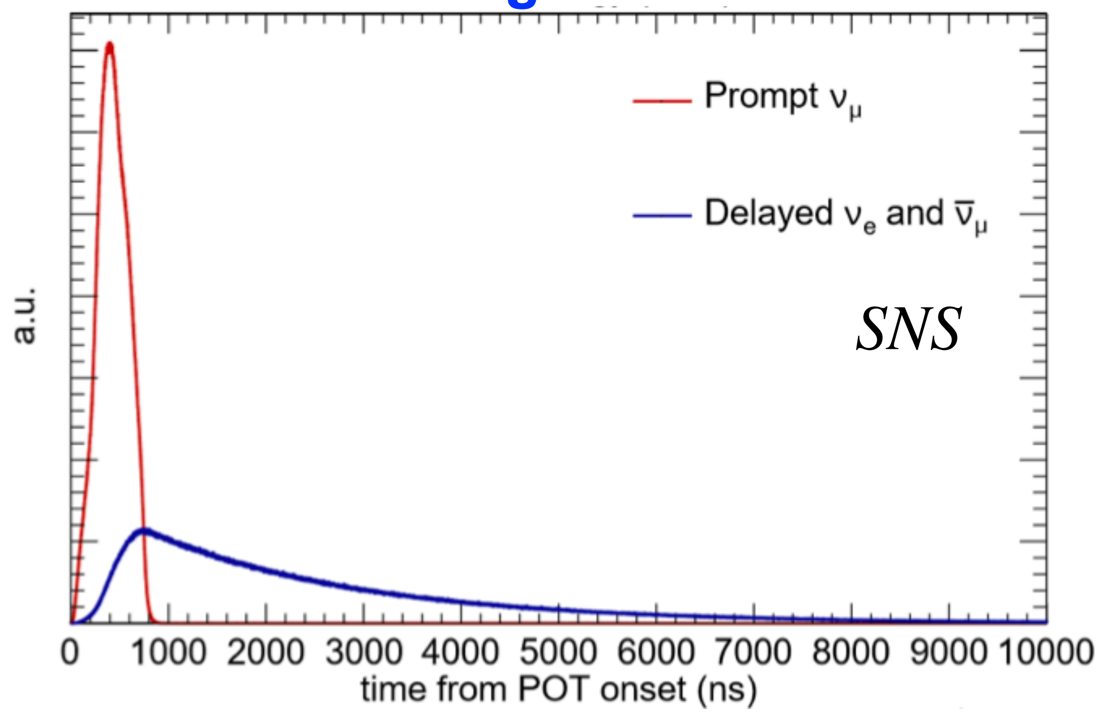

Energy Profile

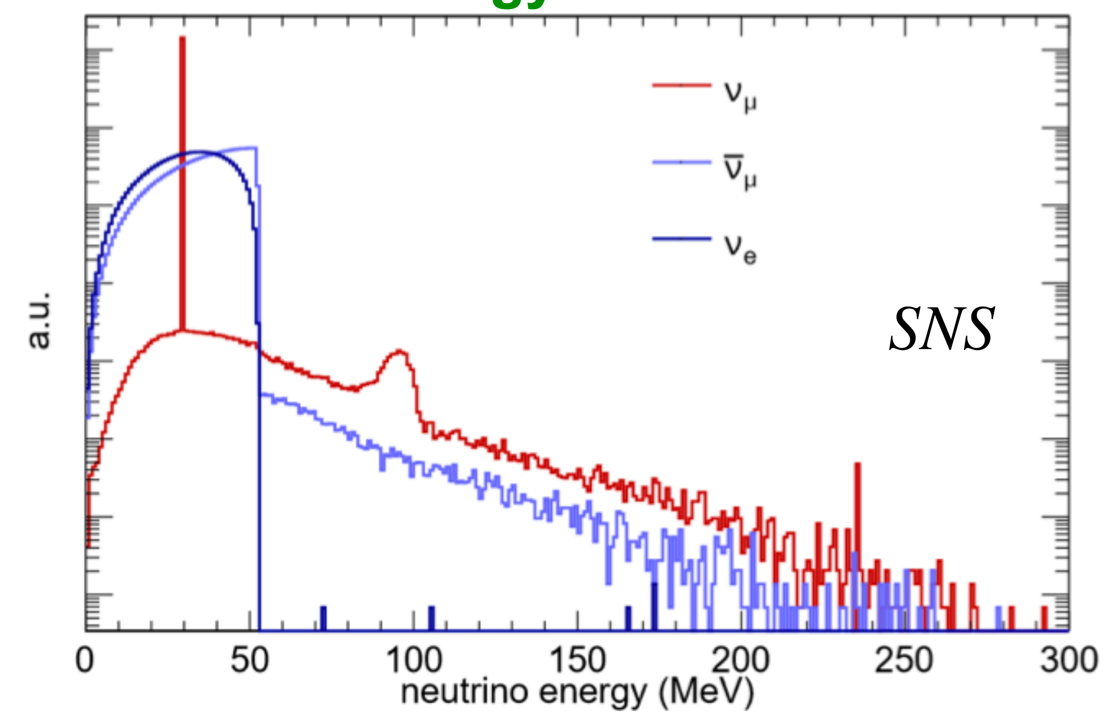

D. Akimov et al. [COHERENT], Science 357, 6356, 1123-1126 (2017)

- Proton pulse duration and time between different pulses are key factors

  - For beam spills < μ^+ lifetime: can separate piDAR and muDAR neutrinos
  - For beam spills < π^+ lifetime: can separate light dark matter production (from π^0, η) from neutrino production

Stopped pion sources and CEvNS

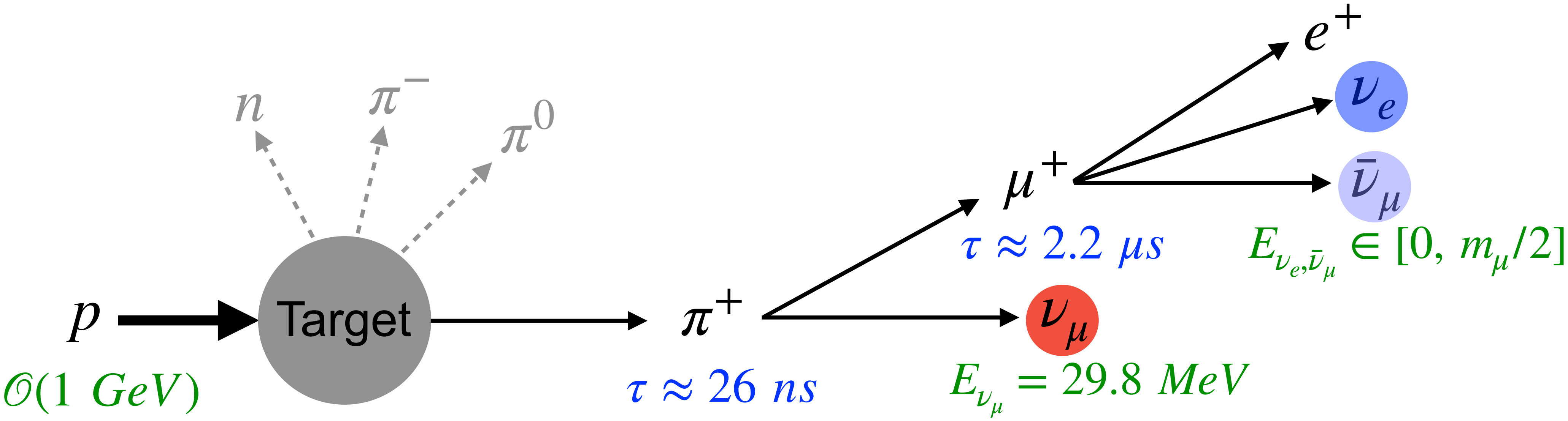

Stopped-Pion Neutrino Sources Worldwide

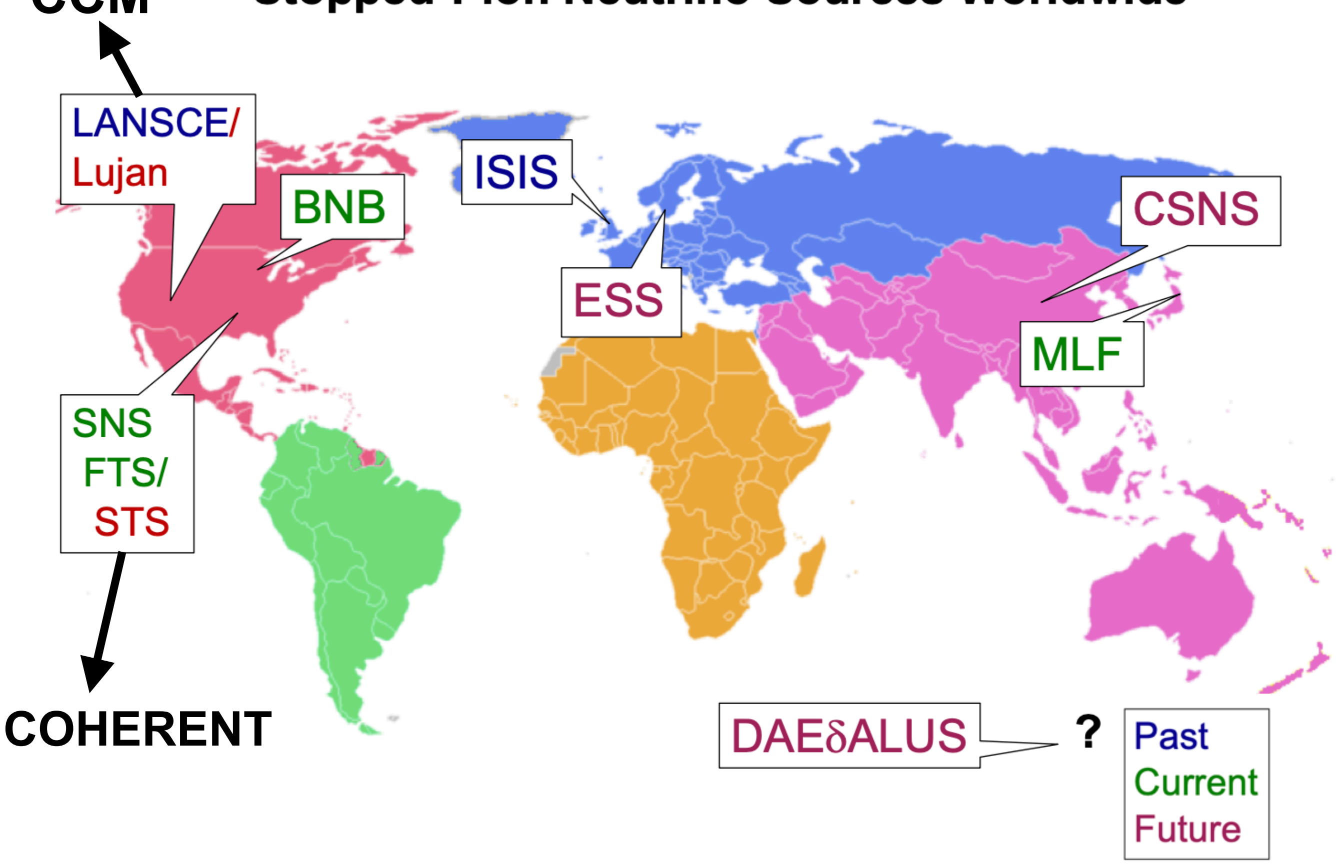

Flavor separation with beam timing can be helpful!

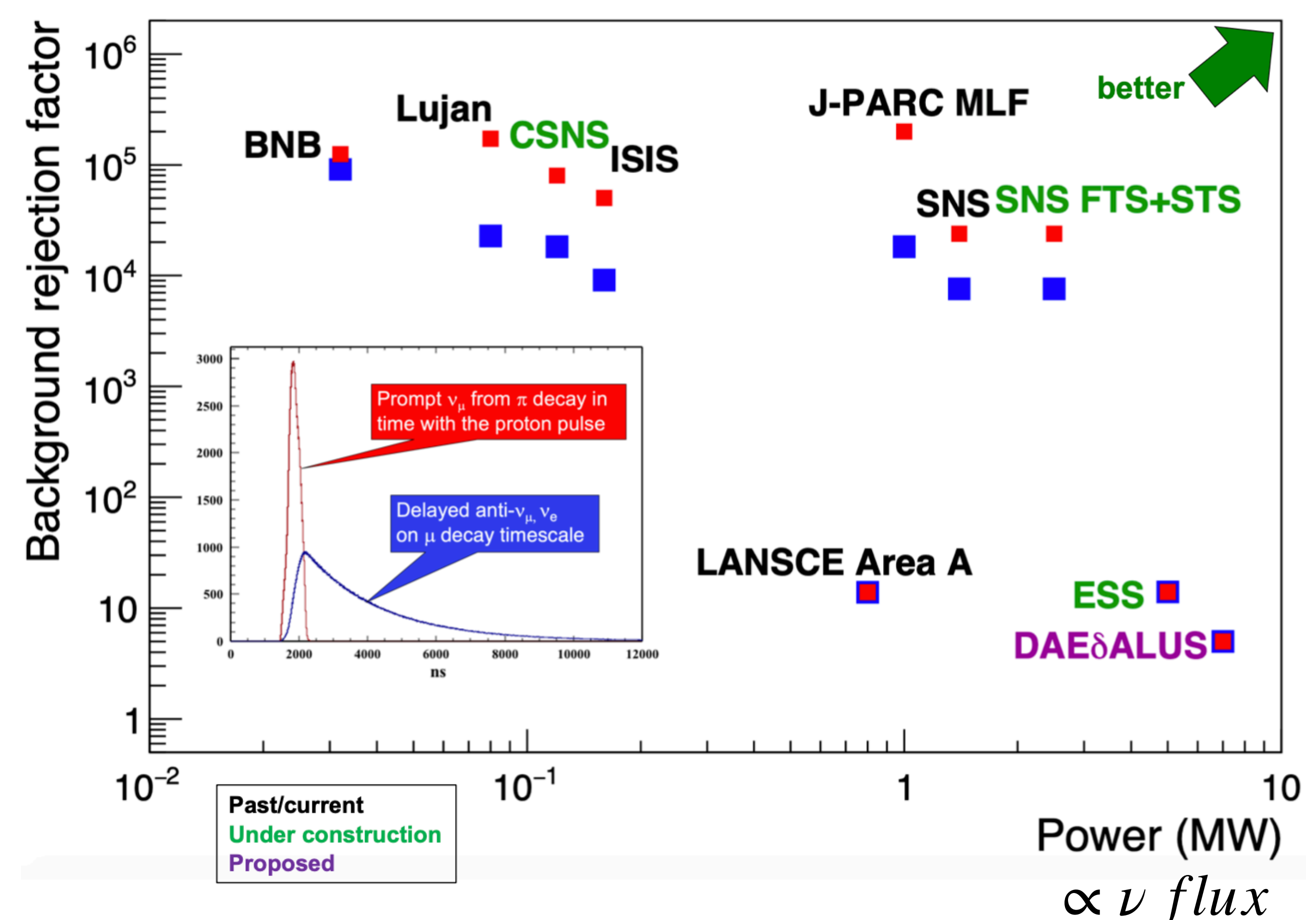

Kate Scholberg, MITP workshop, July 2020

Stopped pion sources and CEvNS

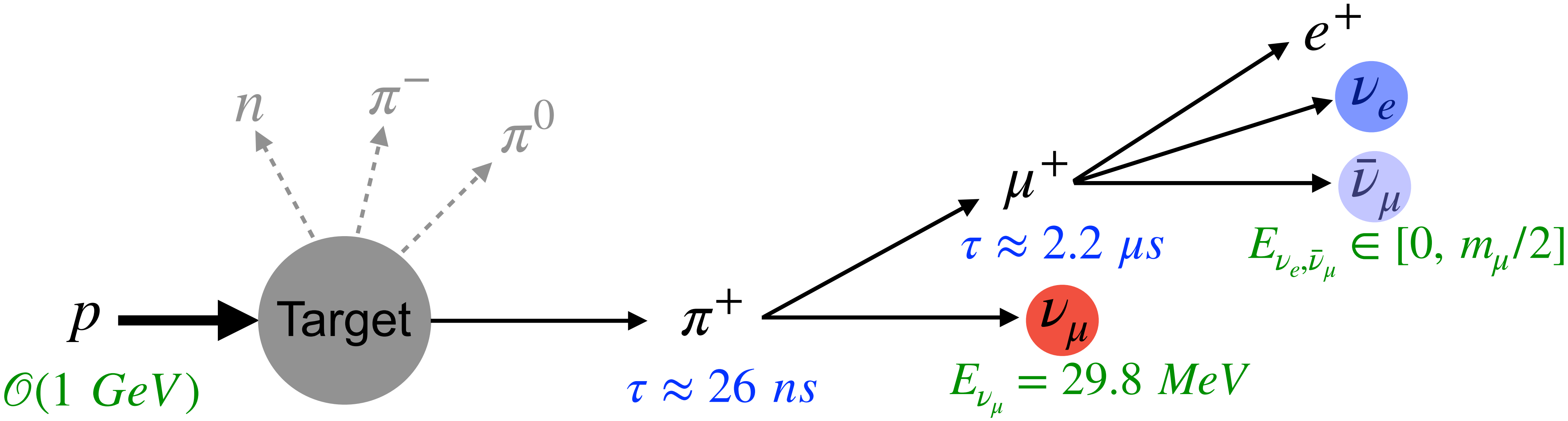

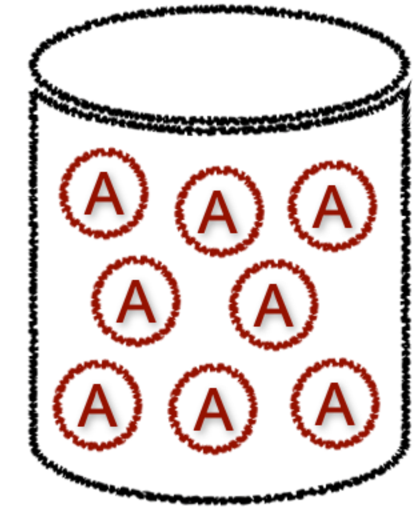

Low threshold (~keV) detector

Coherent elastic neutrino-nucleus scattering (CEvNS):

- Large cross section but tiny recoil
- Only experimental signature: keV energy deposited by nuclear recoil in the target material
- Recent R&D in dark matter and $0\nu\beta\beta$ detector technologies helped overcoming long standing (> 40 years) hurdle

Large cross section

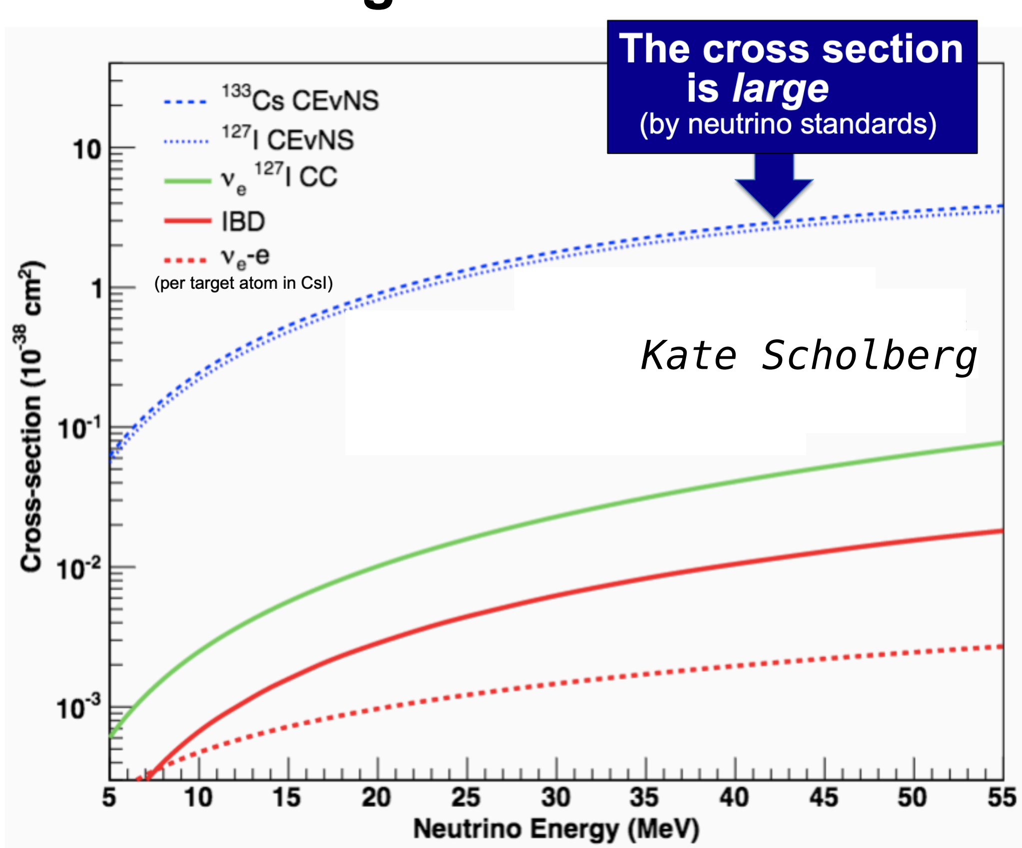

Tiny nuclear recoil

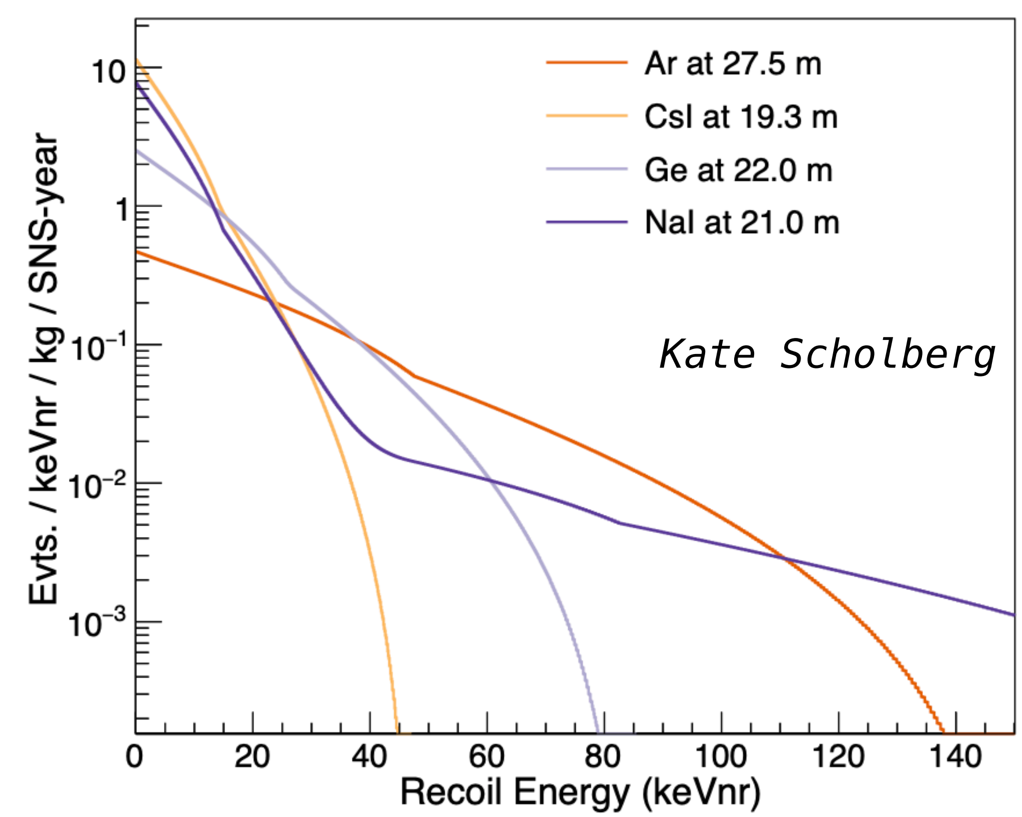

COHERENT Collaboration at SNS at ORNL

- **14 kg CSI detector**

D. Akimov et al. [COHERENT], Science 357, 6356, 1123–1126 (2017)

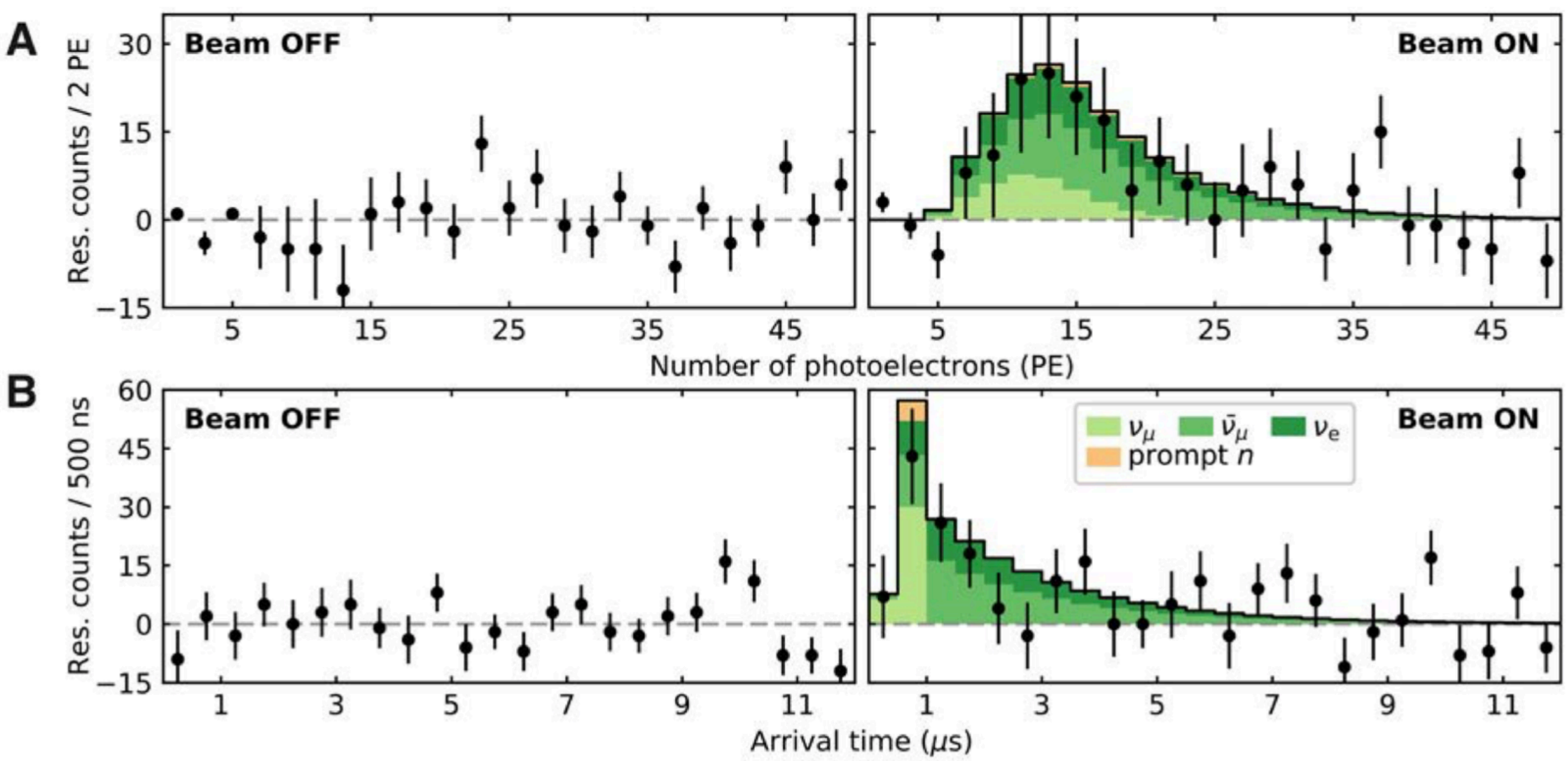

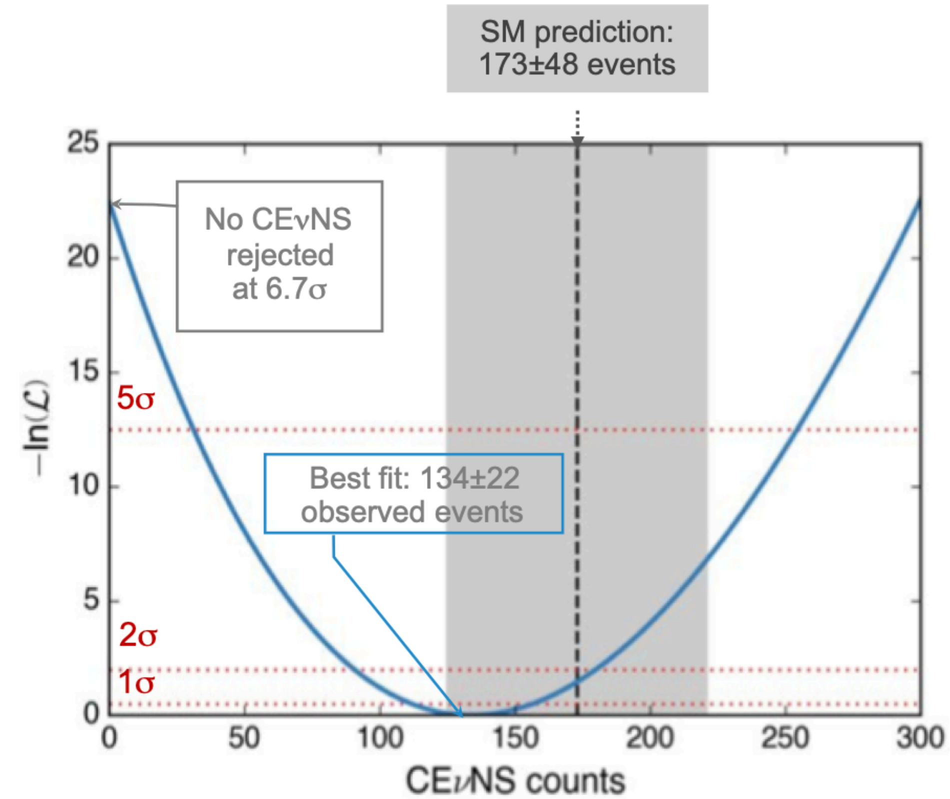

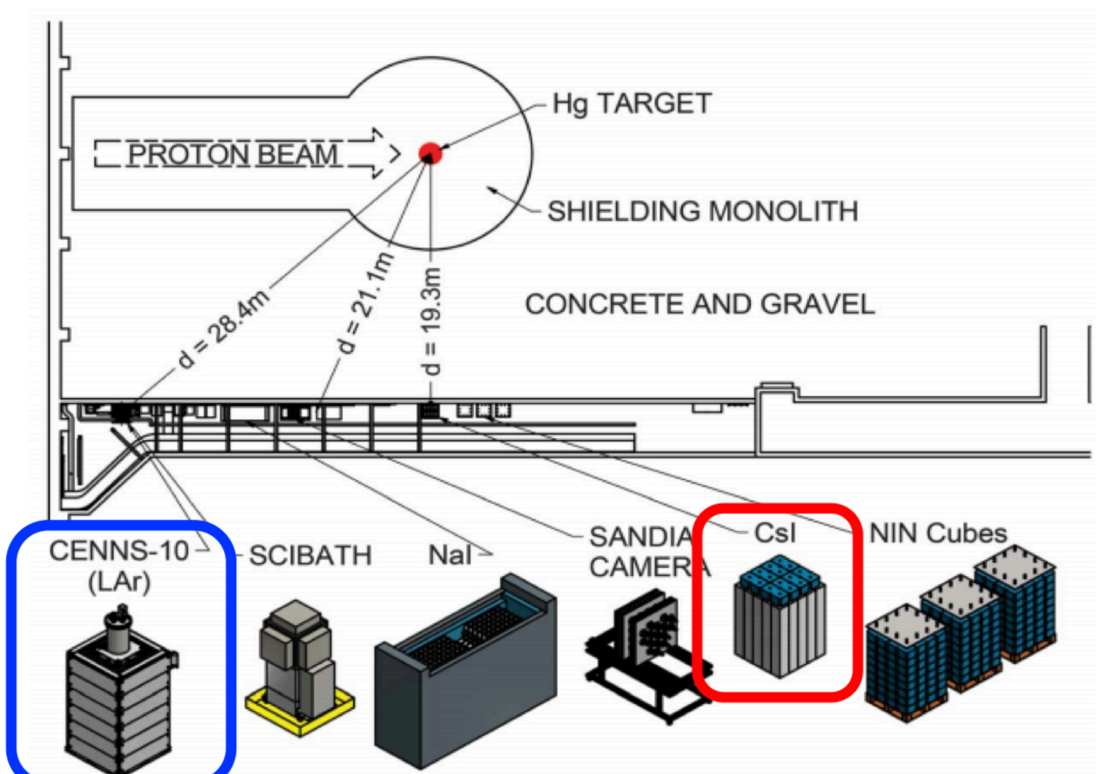

Stopped pion sources and CEvNS

COHERENT Collaboration at SNS at ORNL

- **14 kg CSI detector** *D. Akimov et al. [COHERENT], Science 357, 6356, 1123–1126 (2017)*

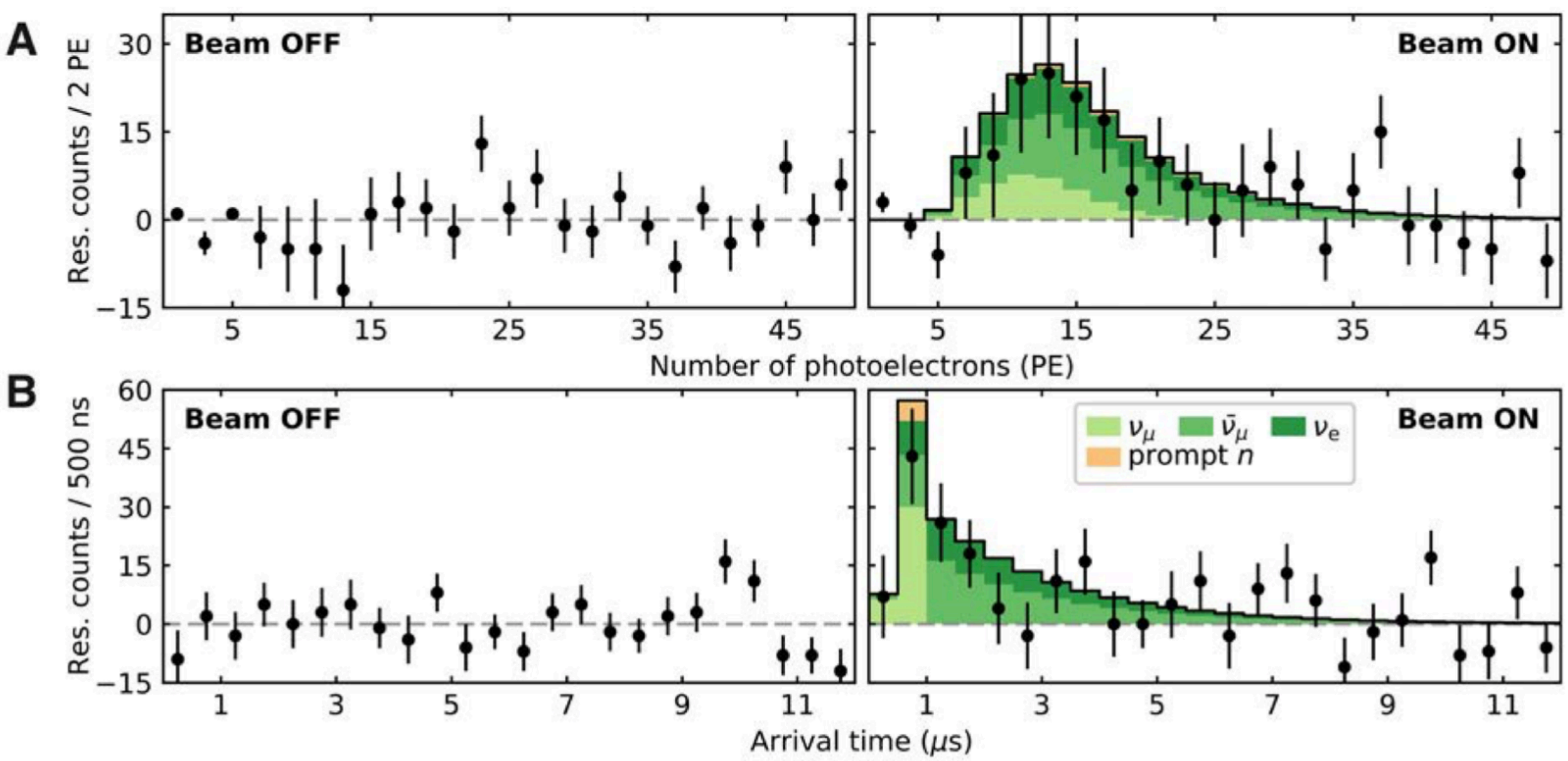

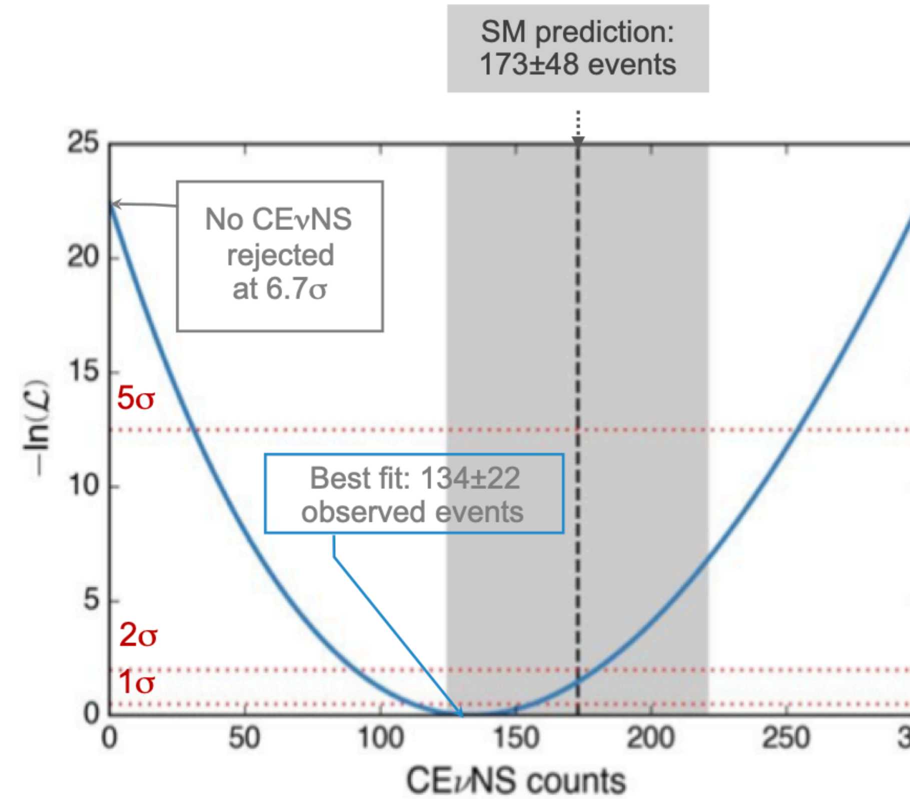

- **24 kg LAr (CENNS-10) detector** *D. Akimov et al. [COHERENT], arXiv:2003.10630 [nucl-ex]*

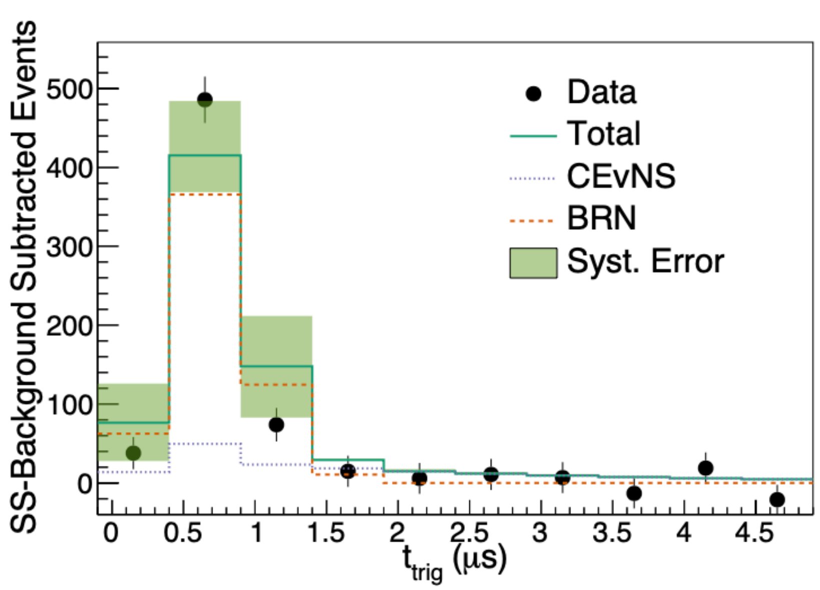

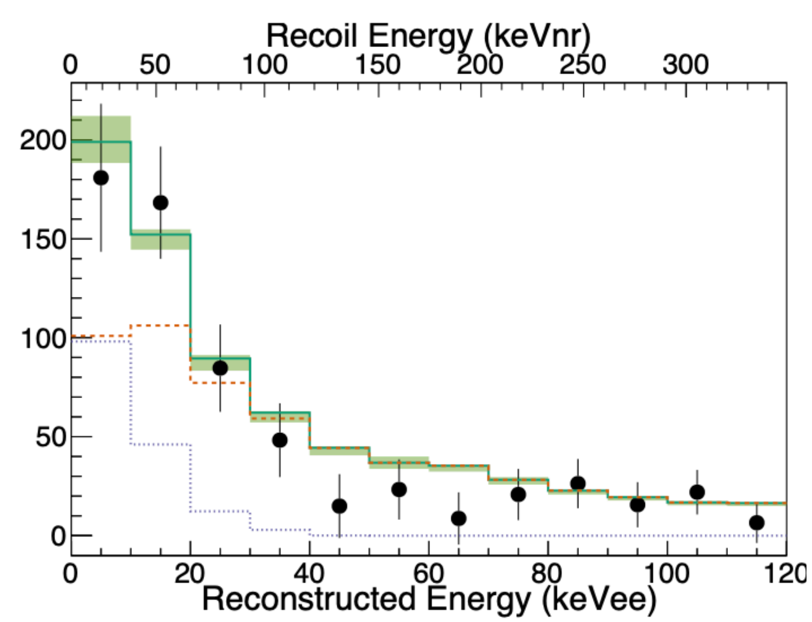

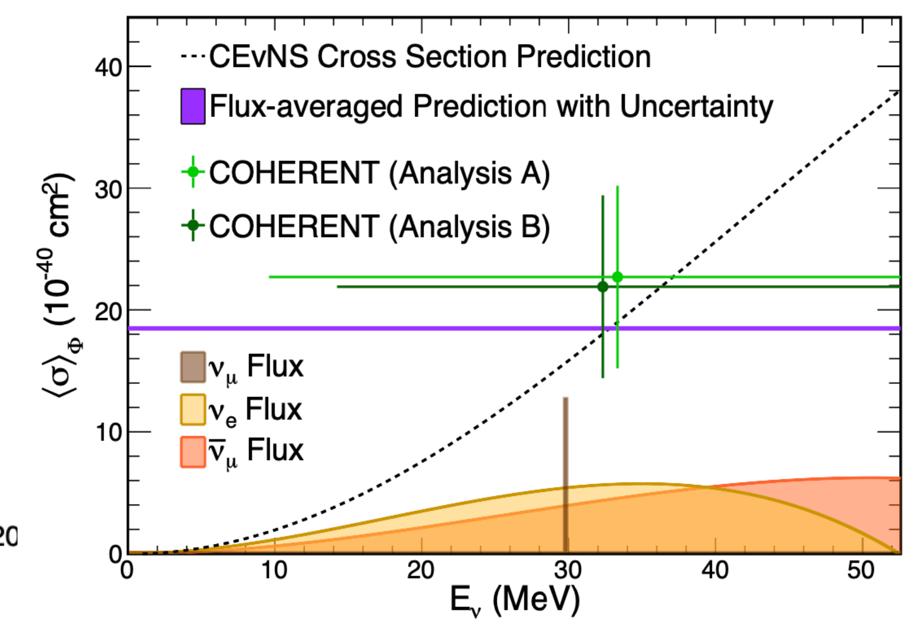

Stopped pion sources and CEvNS

- New physics may be weakly interacting, and hiding at low energies
- Any deviation from the SM expectation → new physics
- SM expectation of CEvNS cross section have to be know at a precision that allows resolving degeneracies in the standard and non-standard physics observables

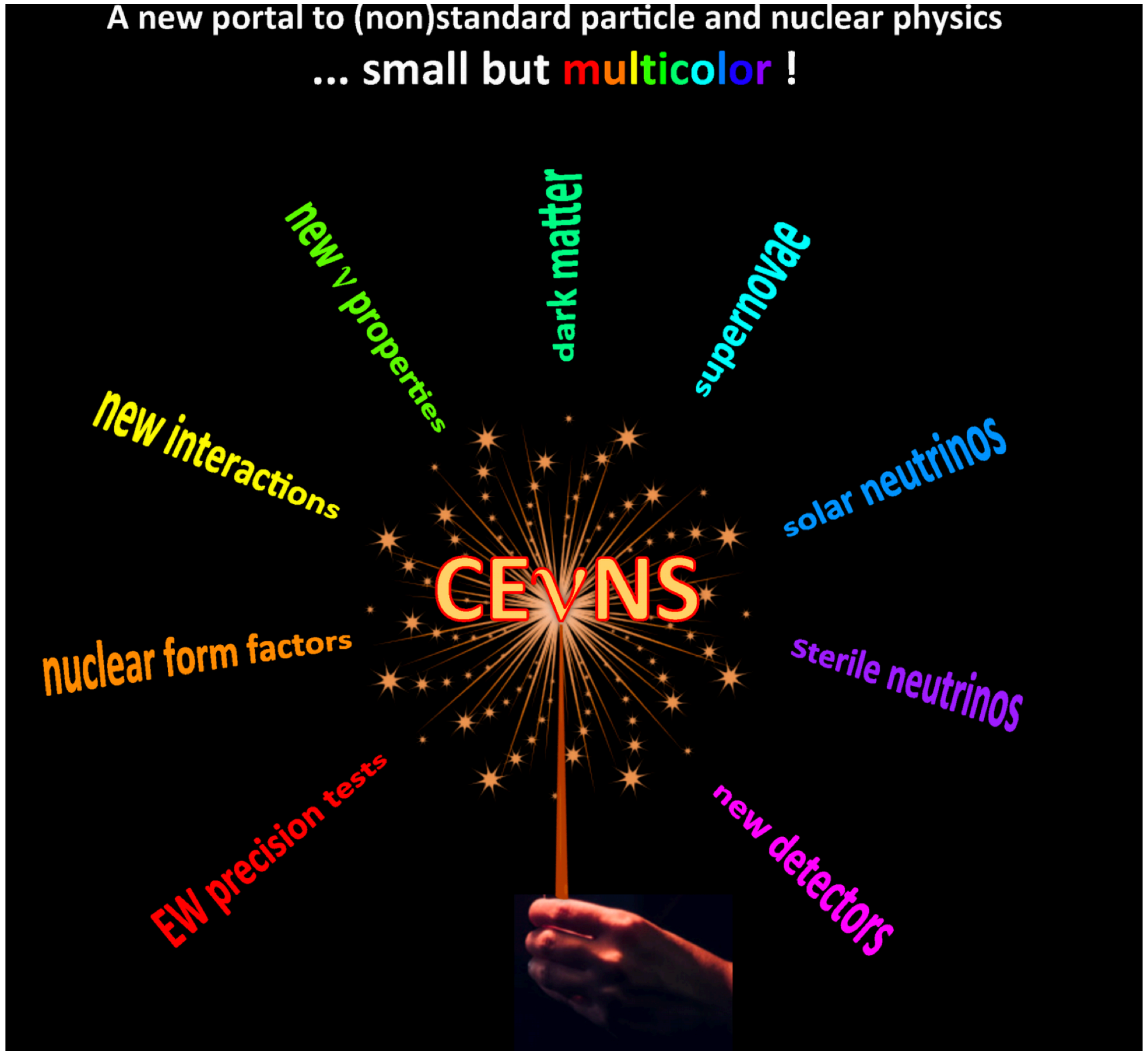

Eligio Lisi, NuINT 2018

Outline

- Stopped pion sources and CEvNS
- **CEvNS formalism: cross section and form factors**
- Nuclear model: HF-SkE2
- Constraining ^{40}Ar
  - Weak form factor and CEvNS cross section
  - Inelastic cross section

CEvNS formalism: cross section and form factors

Kinematics:

$$T = E_i - E_f$$

$$|\vec{q}\,| = |\vec{k}_i - \vec{k}_f|$$

$$|\vec{p}\,'_A| = \sqrt{(M_A + T)^2 - M_A^2}$$

$$q^2 = 2M_A T$$

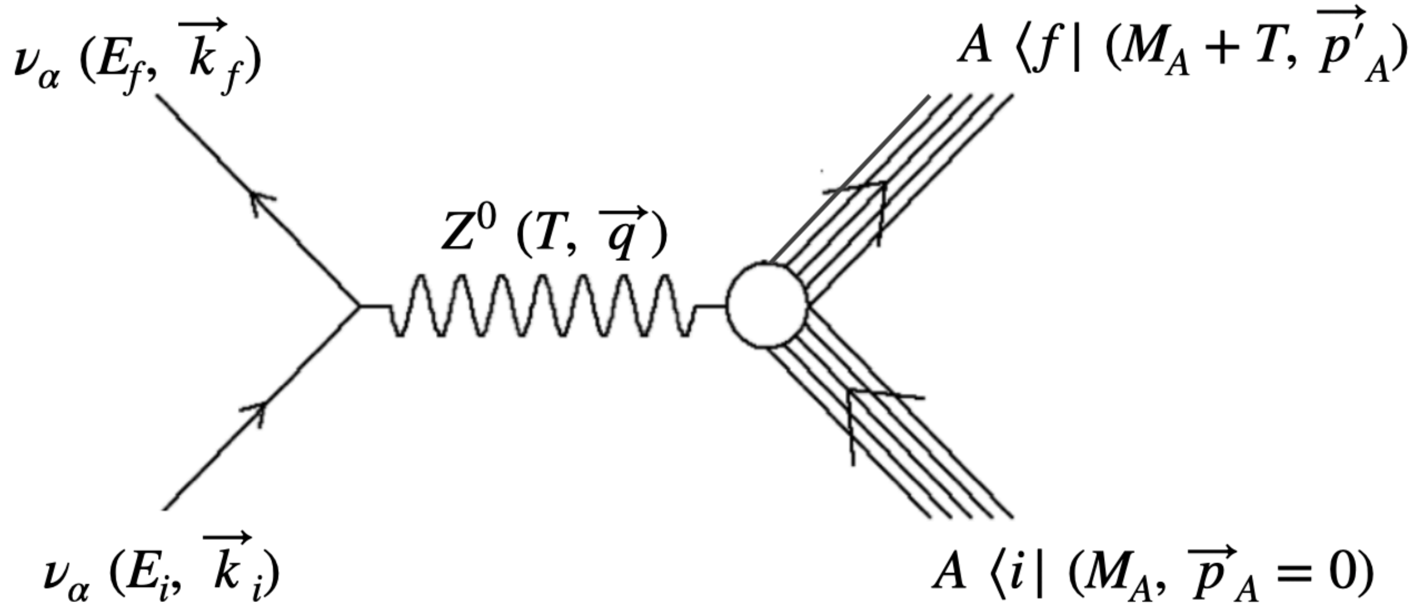

CEvNS formalism: cross section and form factors

Kinematics:

$$T = E_i - E_f$$

$$|\vec{q}\,| = |\vec{k}_i - \vec{k}_f|$$

$$|\vec{p}'_A| = \sqrt{(M_A + T)^2 - M_A^2}$$

$$q^2 = 2M_A T$$

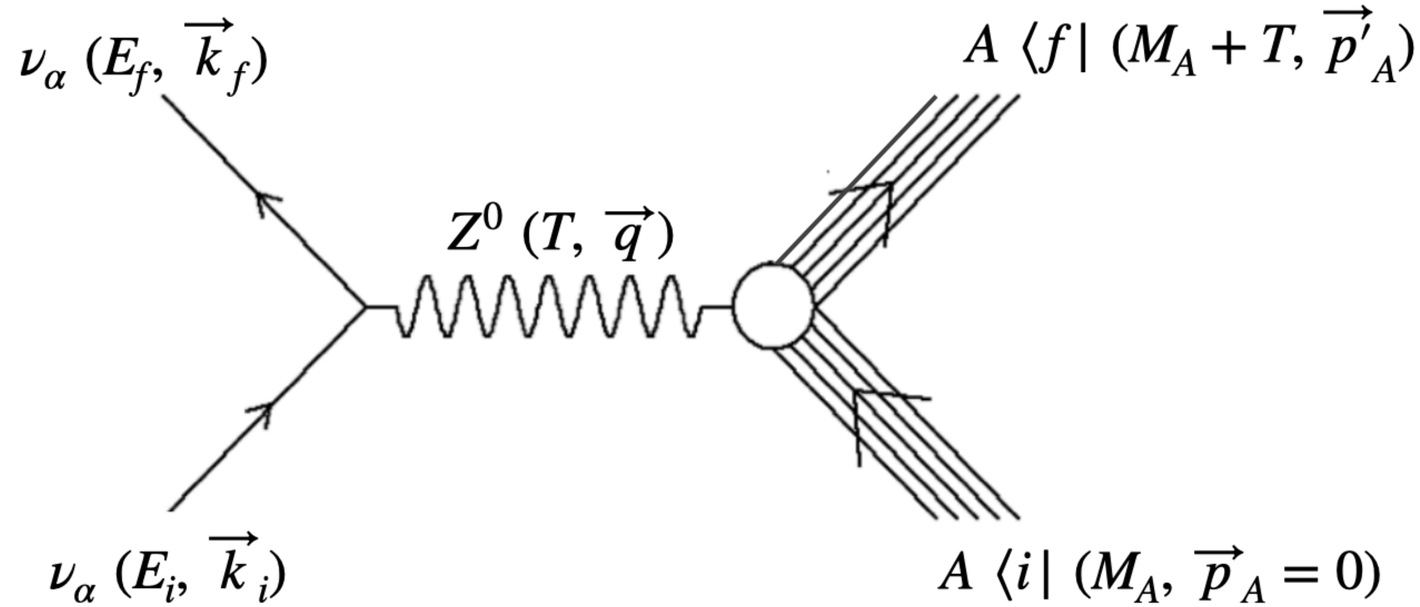

Cross section:

$$\frac{d^6\sigma}{d^3k_f d^3p'_A} \propto \frac{1}{(2\pi)^6} \frac{M_A}{(M_A + T)} \frac{1}{E_i E_F} \times (2\pi)^4 \sum_{fi} |\mathscr{M}|^2 \delta^{(4)}(k_i + p_A - k_f - p'_A)$$

$$\sum_{fi} |\mathscr{M}|^2 \propto \frac{G_F^2}{2} L_{\mu\nu} W^{\mu\nu}$$

Nuclear tensor: $W^{\mu\nu} = \sum_{fi} (\mathscr{J}^\mu_{nucl})^\dagger \mathscr{J}^\nu_{nucl}$

Nuclear current transition amplitude: $\mathscr{J}^\mu_{nucl} = \langle \Phi_0 | \hat{J}^\mu(\vec{q}\,) | \Phi_0 \rangle$

Elastic scattering on a spherically symmetric nuclei ($J^\pi = 0^+$): $\approx \dfrac{Q_W}{2} F_W(q)$

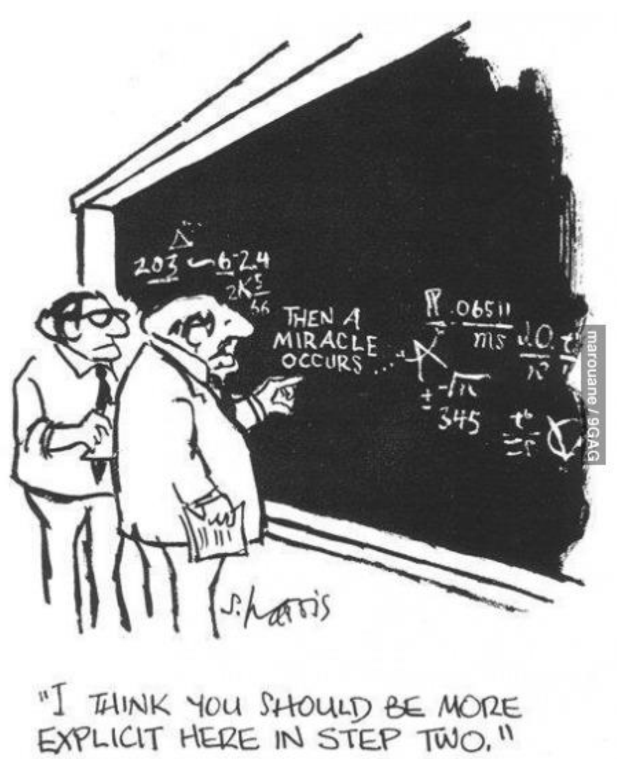

CEvNS formalism: cross section and form factors

Cross section:

$$\boxed{\frac{d\sigma}{dT} = \frac{G_F^2}{\pi} M_A \left[1 - \frac{T}{E_i} - \frac{M_A T}{2E_i^2}\right] \frac{Q_W^2}{4} F_W^2(q)}$$

$$\boxed{\frac{d\sigma}{d\cos\theta_f} = \frac{G_F^2}{2\pi} E_i^2 (1 + \cos\theta_f) \frac{Q_W^2}{4} F_W^2(q)}$$

- Nuclear recoil $$\boxed{T \in \left[0, \frac{2E_i^2}{(M_A + 2E_i)}\right]}$$

- Heavier target nuclei -> larger cross section

- Heavier target nuclei -> smaller recoil energy

- Higher neutrino energy -> higher recoil energy

- Weak nuclear charge $$\boxed{Q_W^2 = [g_n^V N + g_p^V Z]^2 = [N - (1 - 4\sin^2\theta_W)\ Z]^2}$$

Cross section:

$$\frac{d\sigma}{dT} = \frac{G_F^2}{\pi} M_A \left[1 - \frac{T}{E_i} - \frac{M_A T}{2E_i^2}\right] \frac{Q_W^2}{4} F_W^2(q)$$

$$\frac{d\sigma}{d\cos\theta_f} = \frac{G_F^2}{2\pi} E_i^2 (1 + \cos\theta_f) \frac{Q_W^2}{4} F_W^2(q)$$

- In CEvNS process, the entire nuclear structure and dynamics is encoded in the weak form factor $F_W(q)$.

$$F_W(q) = \frac{1}{Q_W}\left[\left(1 - 4\sin^2\theta_W\right) Z\, F_p(q) - N\, F_n(q)\right]$$

$$F_W(q) = \frac{4\pi}{Q_W}\int d^3r\, \left[(1 - 4\sin^2\theta_W)\, \rho_p(r) - \rho_n(r)\right] j_0(qr)$$

Charge density and charge form factor: proton densities and charge form factors are well constrained through decades of elastic electron scattering experiments.

Neutron densities and neutron form factor: neutron densities and form factors are poorly known. Note that CEvNS is primary sensitive to neutron density distributions.

CEvNS formalism: cross section and form factors

■ Neutron densities and form factor

- **Hadronic probes** have been used to extract neutron distributions but these measurements are plagued by ill-controlled model–dependent uncertainties associated with the strong interaction.

- **Electroweak probes** such as parity–violating electron scattering (**PVES**) and **CEvNS** provide relatively model-independent ways of determining neutron distributions.

CEvNS formalism: cross section and form factors

Neutron densities and form factor

- **Hadronic probes** have been used to extract neutron distributions but these measurements are plagued by ill-controlled model–dependent uncertainties associated with the strong interaction.

- **Electroweak probes** such as parity–violating electron scattering (**PVES**) and **CEvNS** provide relatively model-independent ways of determining neutron distributions.

  - **PVES experiments:** In recent years, PREX experiment at Jefferson lab has measured the weak charge of ^{208}Pb at a single value of momentum transfer, while a follow up PREX–II experiment is underway. CREX experiment at Jefferson lab is underway to measure the weak form factor of ^{48}Ca.

$$\boxed{A_{PV}(q^2) = \frac{G_F q^2}{4\pi\alpha\sqrt{2}} \frac{Q_W F_W(q^2)}{Z F_{ch}(q^2)}}$$

  - **CEvNS experiments:** Ton and multi-ton CEvNS detectors will enable more precise measurements and will potentially offer a powerful avenue to constrain neutron density distributions and weak form factors of nuclei at low momentum transfers.

$$\boxed{\frac{d\sigma}{dT} = \frac{G_F^2}{4\pi} M_A \left[1 - \frac{T}{E_i} - \frac{M_A T}{2E_i^2}\right] Q_W^2 F_W^2(q)}$$

CEvNS formalism: cross section and form factors

- With no experimental data to constrain neutron distributions and weak nuclear form factors, these have to be modeled in order to evaluate the CEvNS cross section and event rates.

  A. Microscopic many-body nuclear theory approaches that describe more accurate picture of the nuclear ground state and nucleon densities.

  B. Phenomenological approaches where density distributions are represented by analytical expressions, widely used in the CEvNS community.

  One can assume: $\rho_n(r) \approx \rho_p(r)$ and hence $F_n(q) \approx F_p(q) \approx F_A(q)$

CEvNS formalism: cross section and form factors

- With no experimental data to constrain neutron distributions and weak nuclear form factors, these have to be modeled in order to evaluate the CEvNS cross section and event rates.

A. Microscopic many-body nuclear theory approaches that describe more accurate picture of the nuclear ground state and nucleon densities.

- The HF–SkE2 model (this work arXiv:2007.03658 [nucl-th])
- ………
- ………
- ………

B. Phenomenological approaches where density distributions are represented by analytical expressions, widely used in the CEvNS community.

One can assume: $\rho_n(r) \approx \rho_p(r)$ and hence $F_n(q) \approx F_p(q) \approx F_A(q)$

- The Helm approach
- The Klein–Nystrand (KN) approach (adapted by the COHERENT collaboration)

Outline

- Stopped pion sources and CEvNS
- CEvNS formalism: cross section and form factors
- **Nuclear model: HF-SkE2**
- Constraining ^{40}Ar
  - Weak form factor and CEvNS cross section
  - Inelastic cross section

HF-SkE2 (Ghent) Model

- A microscopic many–body nuclear theory model.
- Nuclear ground state is described as a many-body quantum mechanical system where nucleons are bound in a realistic nuclear potential.
- Solve Hartree-Fock (**HF**) equation with a Skyrme (**SkE2**) nuclear potential to obtain single–nucleon wave functions for the bound nucleons in the nuclear ground state. Fill up nuclear shells following Pauli principle.
- Evaluate proton and neutron density distributions from those wave functions:

$$\boxed{\rho_\tau(r) = \frac{1}{4\pi r^2} \sum_\alpha v^2_{\alpha,\tau}\,(2j_\alpha + 1)\,|\,\phi_{\alpha,\tau}(r)\,|^2} \quad (\tau = p, n)$$

$$(\alpha \in n_\alpha, l_\alpha, j_\alpha)$$

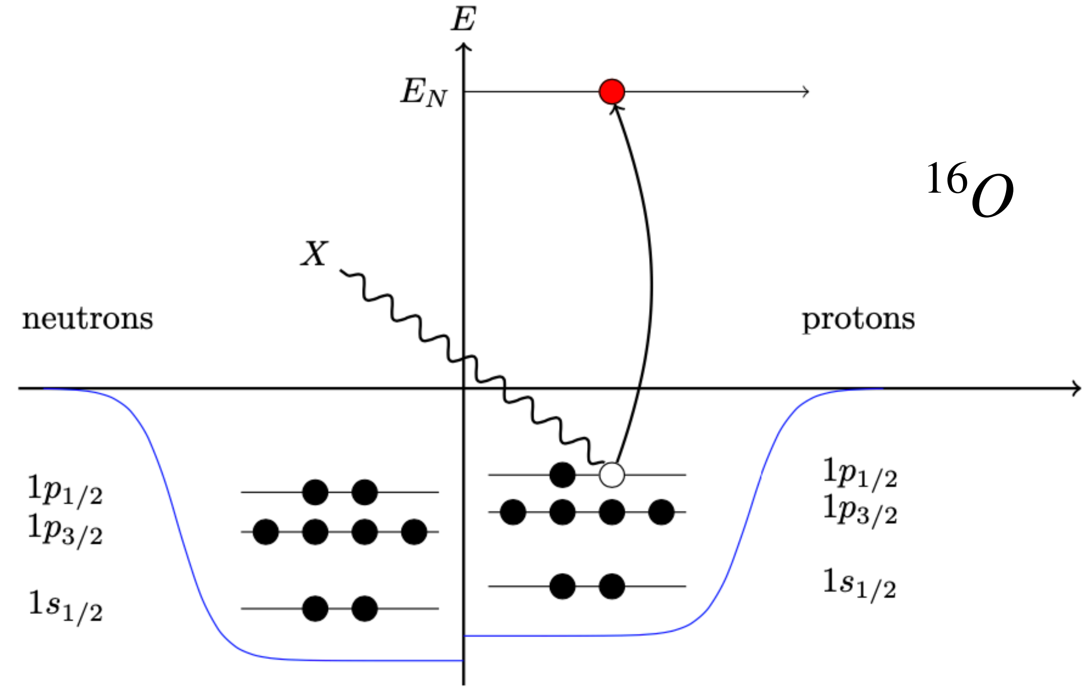

- Approach has been developed and tested against several electron- and neutrino-nucleus scattering datasets and works well for low-energy and QE processes at MiniBooNE/MicroBooNE/T2K kinematics.

Phys. Rev. Lett. 123, 052501 (2019)
Phys. Rev. C 97, 044616 (2018)
Phys. Rev. C 94, 054609 (2016)
Phys. Rev. C 92, 024606 (2015)
Phys. Rev. C 89, 024601 (2014)
……

- A microscopic many–body nuclear theory model.
- Nuclear ground state is described as a many-body quantum mechanical system where nucleons are bound in a realistic nuclear potential.
- Solve Hartree-Fock (**HF**) equation with a Skyrme (**SkE2**) nuclear potential to obtain single–nucleon wave functions for the bound nucleons in the nuclear ground state. Fill up nuclear shells following Pauli principle.
- Evaluate proton and neutron density distributions from those wave functions:

$$\boxed{\rho_\tau(r) = \frac{1}{4\pi r^2}\sum_\alpha v^2_{\alpha,\tau}\,(2j_\alpha + 1)\,|\,\phi_{\alpha,\tau}(r)\,|^2} \quad (\tau = p, n)$$

$$(\alpha \in n_\alpha, l_\alpha, j_\alpha)$$

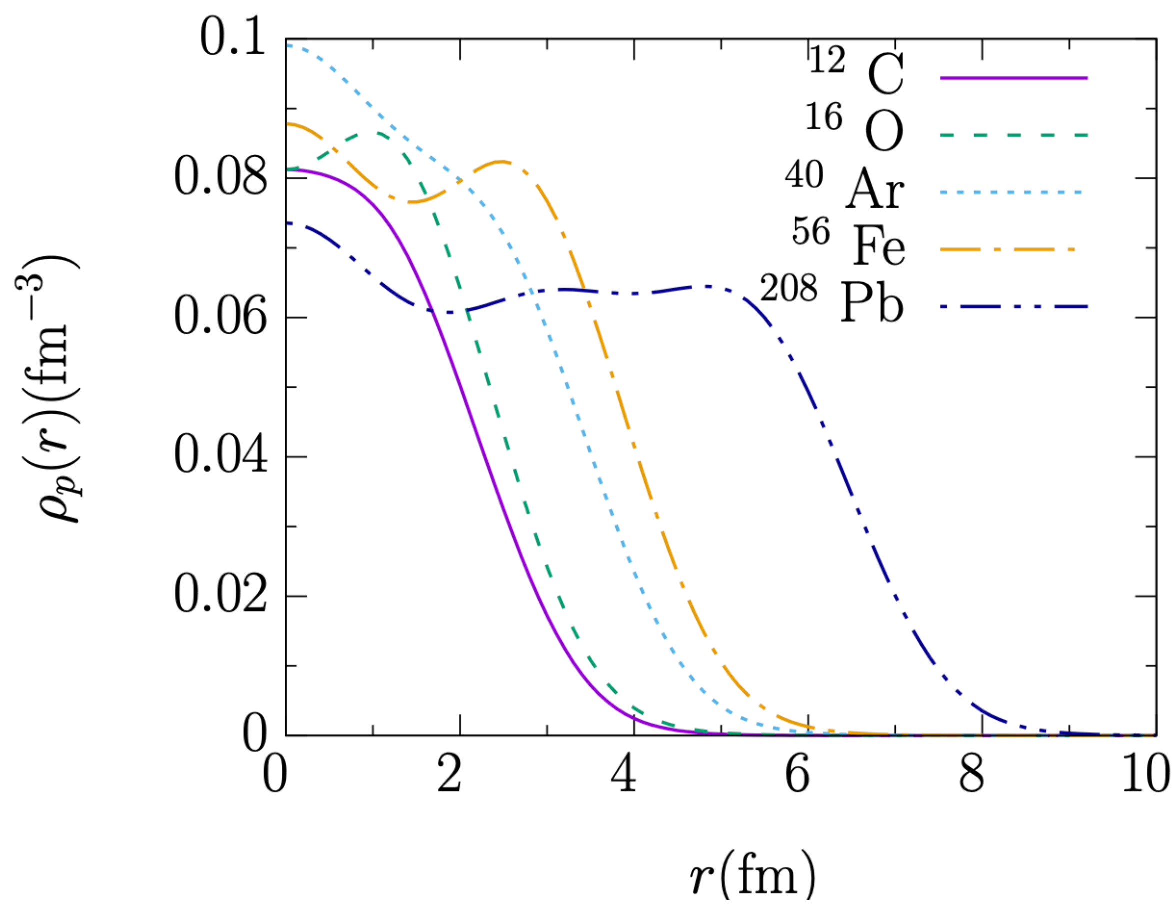

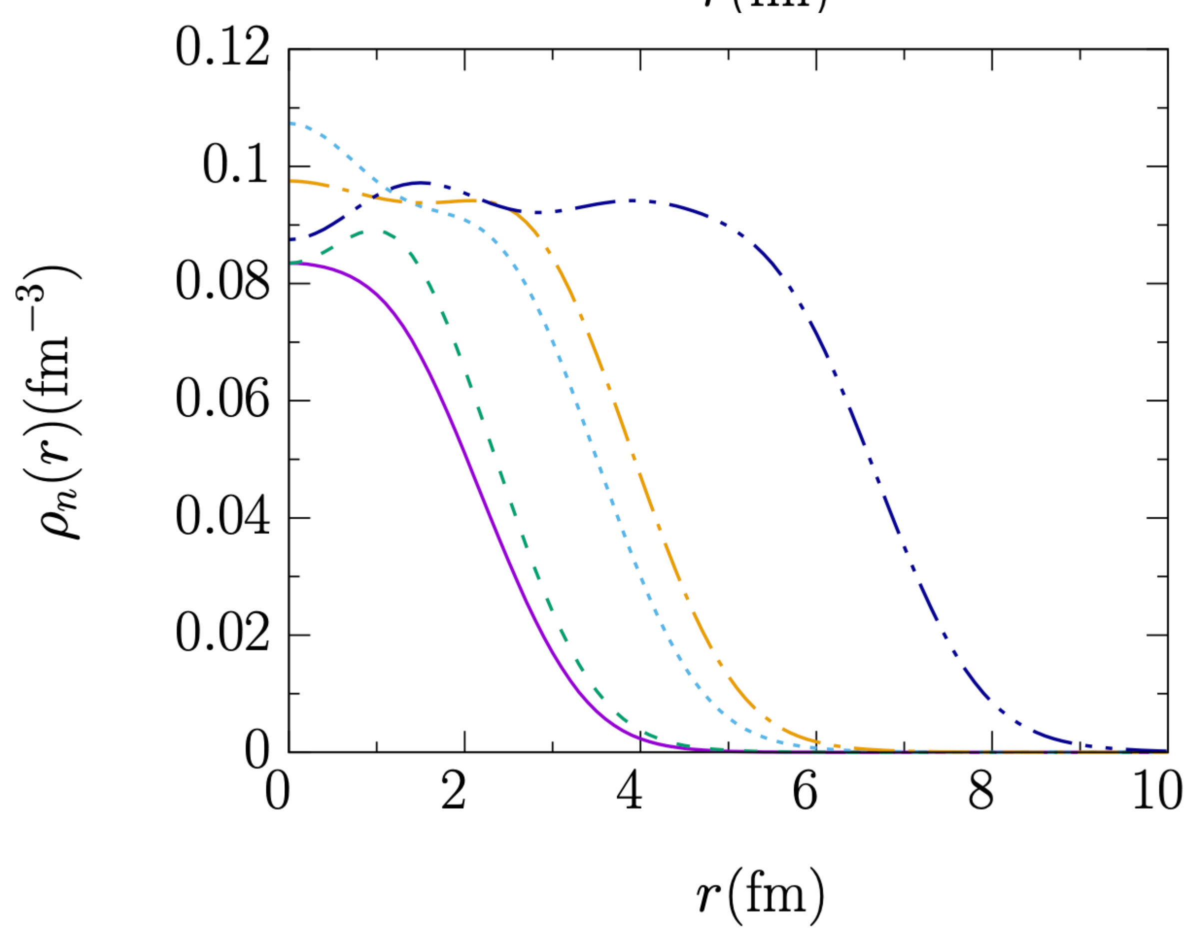

HF-SkE2 (Ghent) Model

- A microscopic many–body nuclear theory model.
- Nuclear ground state is described as a many-body quantum mechanical system where nucleons are bound in a realistic nuclear potential.
- Solve Hartree-Fock (**HF**) equation with a Skyrme (**SkE2**) nuclear potential to obtain single–nucleon wave functions for the bound nucleons in the nuclear ground state. Fill up nuclear shells following Pauli principle.
- Evaluate proton and neutron density distributions from those wave functions:

$$\boxed{\rho_\tau(r) = \frac{1}{4\pi r^2} \sum_\alpha v_{\alpha,\tau}^2 \, (2j_\alpha + 1) \, |\phi_{\alpha,\tau}(r)|^2} \quad (\tau = p, n)$$

$$(\alpha \in n_\alpha, l_\alpha, j_\alpha)$$

- The proton and neutron densities are utilized to calculate proton and neutron form factors:

$$F_n(q) = \frac{1}{N} \int d^3r \, j_o(qr) \, \rho_n(r) \qquad N = \int d^3r \, \rho_n(r)$$

$$F_p(q) = \frac{1}{Z} \int d^3r \, j_o(qr) \, \rho_p(r) \qquad Z = \int d^3r \, \rho_p(r)$$

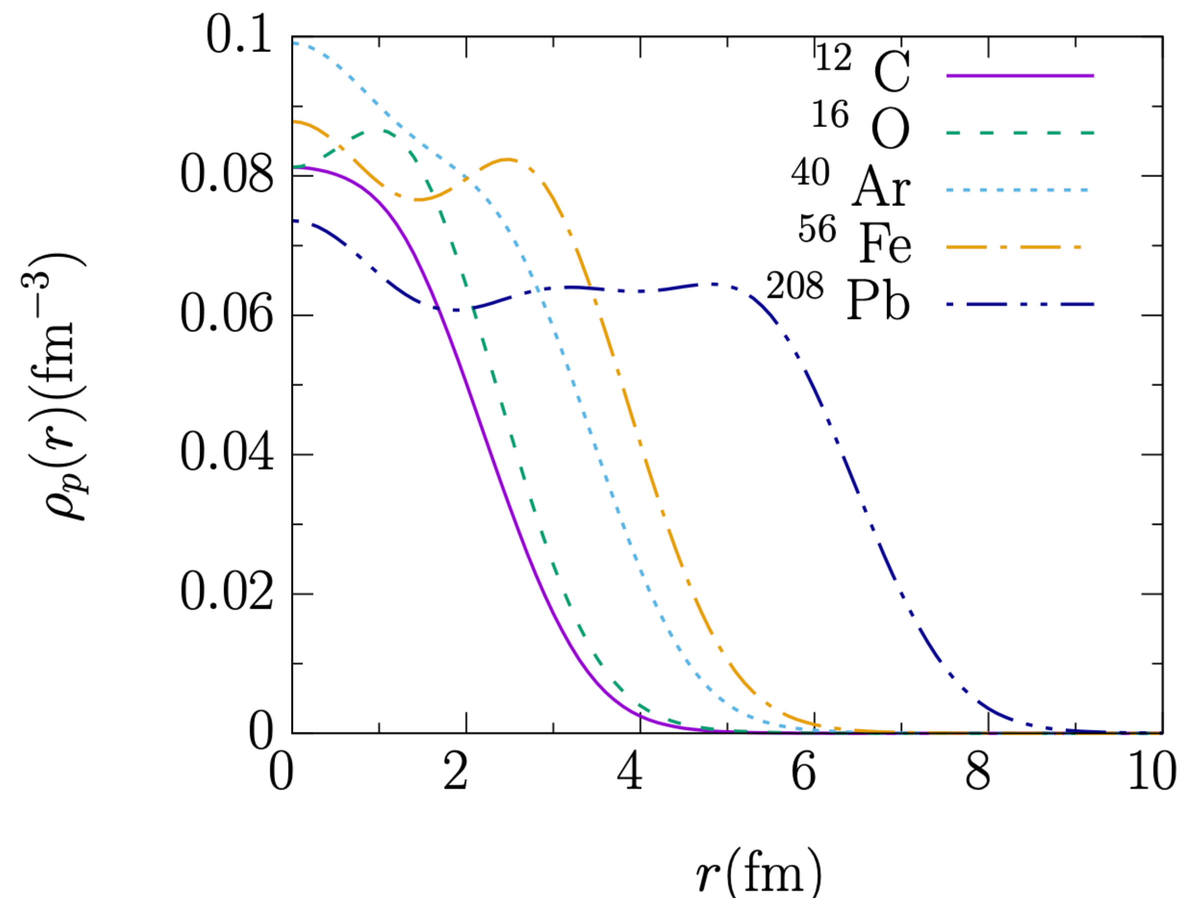

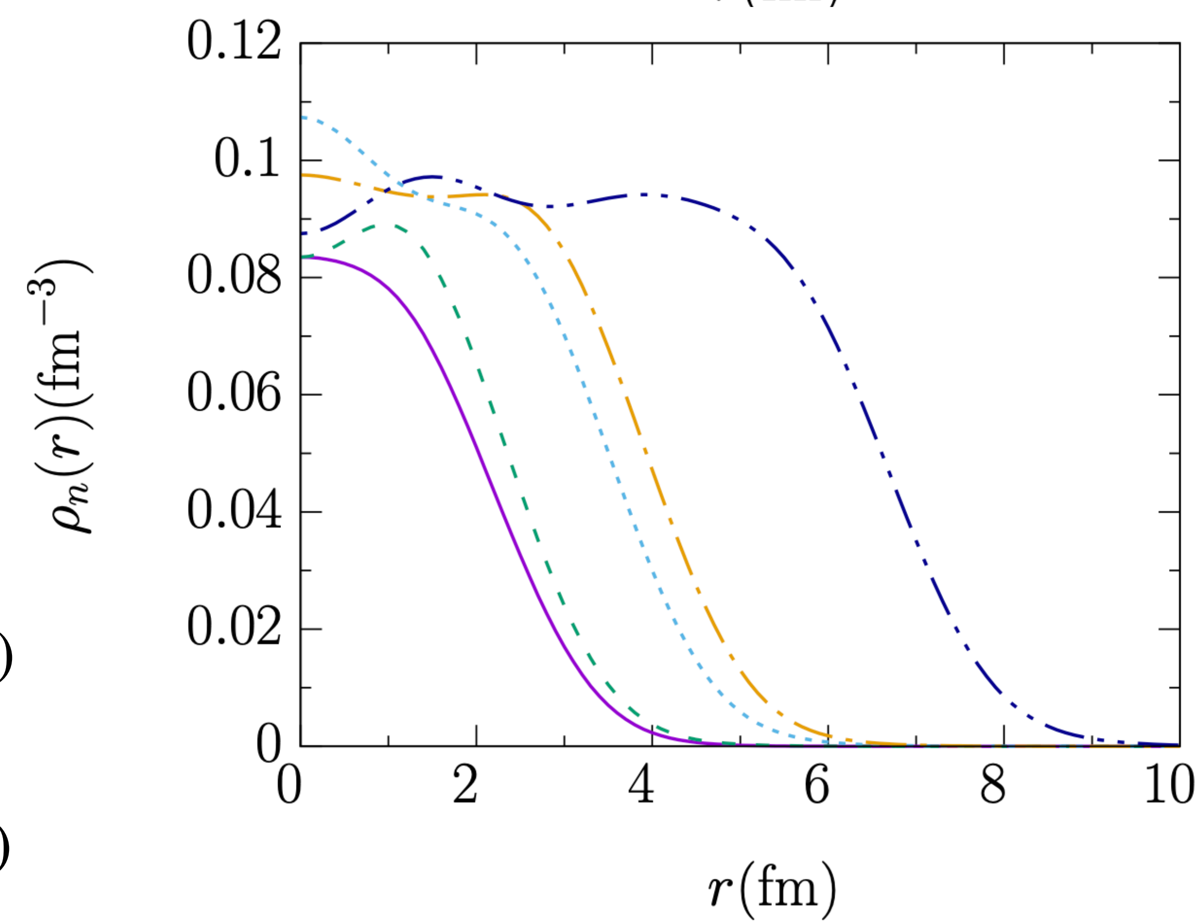

HF-SkE2 Model: ^{208}Pb Results

- **Charge Form Factor**

  - Our charge form factor predictions of ^{208}Pb describe the elastic electron scattering experimental data remarkably well.

Experimental data from:
H. De Vries, et al., Atom. Data Nucl. Data Tabl. 36, 495 (1987)

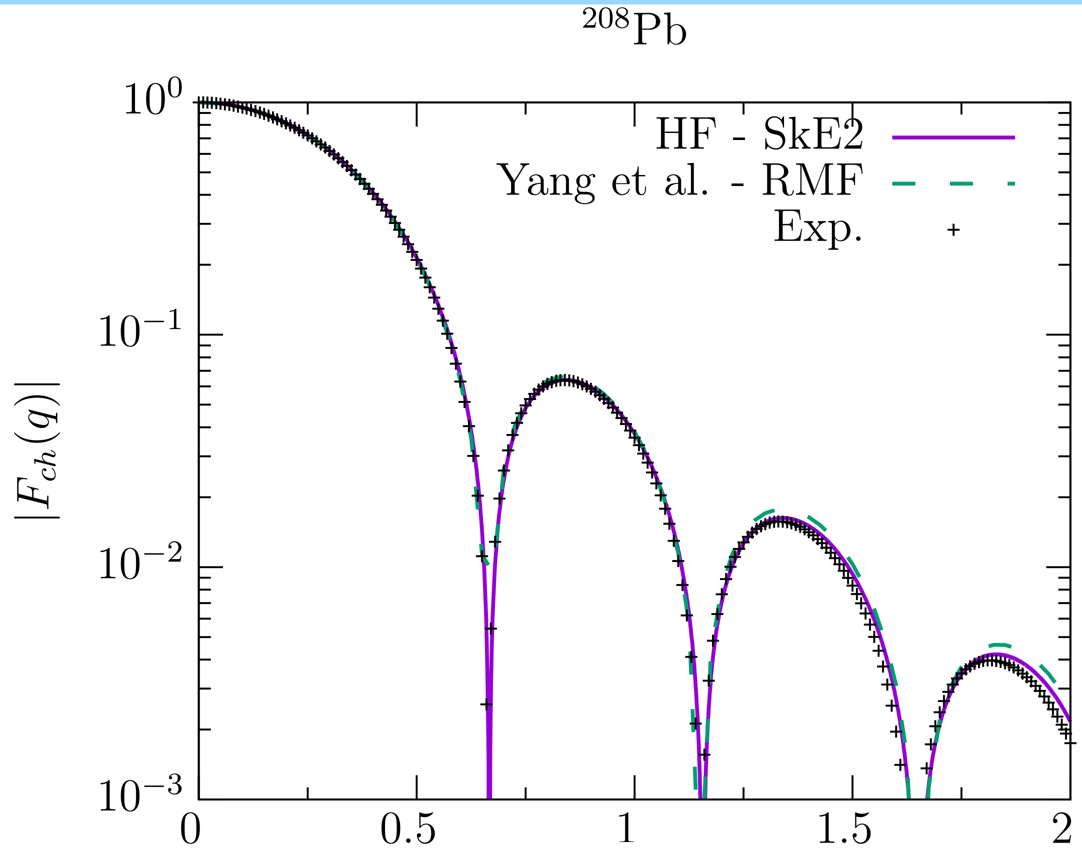

HF-SkE2 Model: ^{208}Pb Results

- **Charge Form Factor**
  - Our charge form factor predictions of ^{208}Pb describe the elastic electron scattering experimental data remarkably well.

Experimental data from:
H. De Vries, et al., Atom. Data Nucl. Data Tabl. 36, 495 (1987)

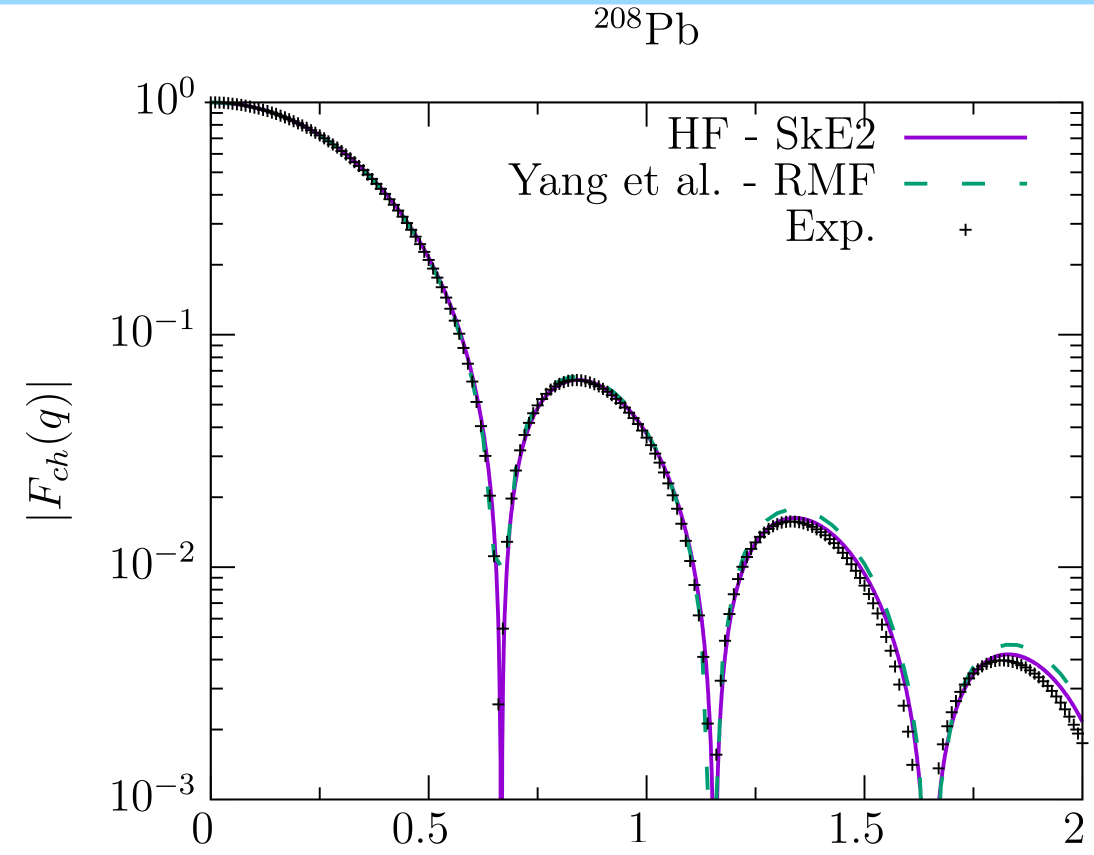

- **Weak Form Factor**
  - Weak form factor predictions shown along with the single data point measured by the PREX collaboration at a momentum transfer of q = 0.475 fm^{-1}.
  - The follow–up PREX–II measurement at Jefferson lab aims to reduce the error bars by at least a factor of three.

PREX data from:
- S. Abrahamyan et al., Phys. Rev. Lett. 108, 112502 (2012).
- C. J. Horowitz et al., Phys. Rev. C 85, 032501 (2012).

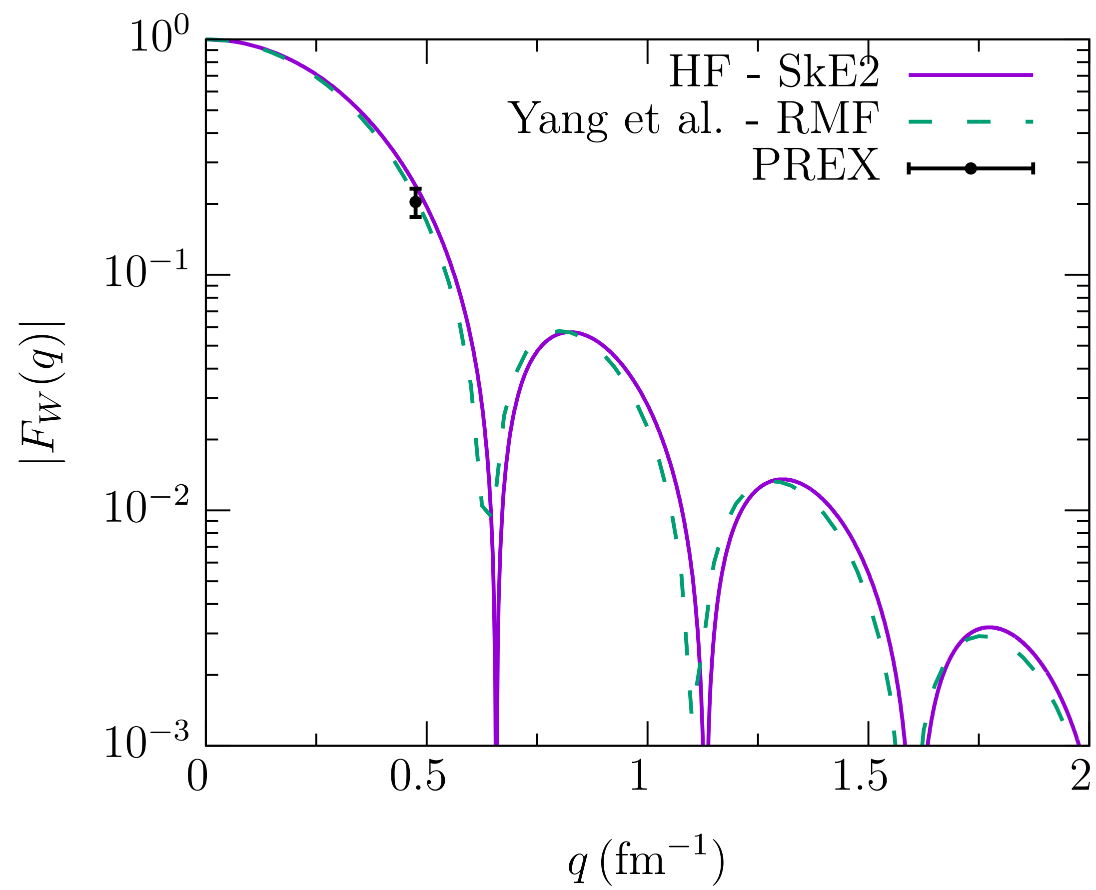

- Both calculations compared with RMF predictions of Yang *et al. (Phys. Rev. C 100, 054301 (2019))*.

HF-SkE2 Model: ^{208}Pb Results

- **Weak-skin Form Factor**

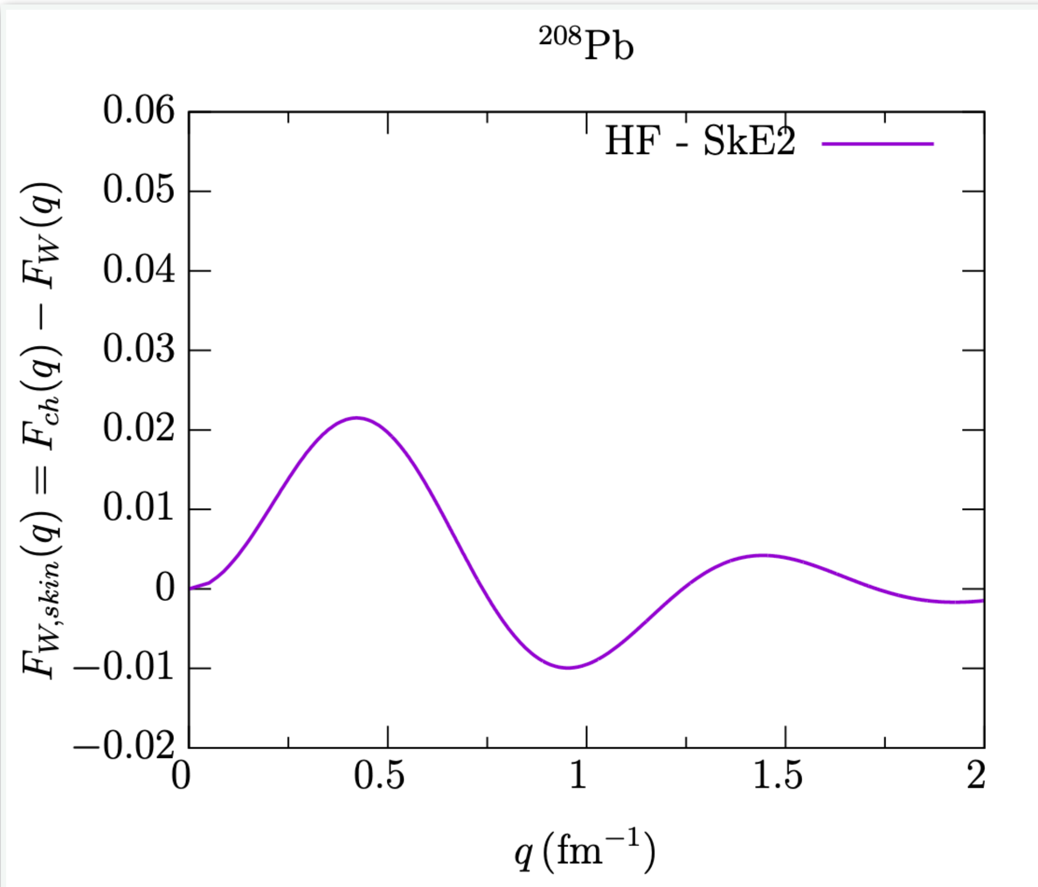

- The “weak-skin” form factor depicts the difference between the charge and weak form factors.

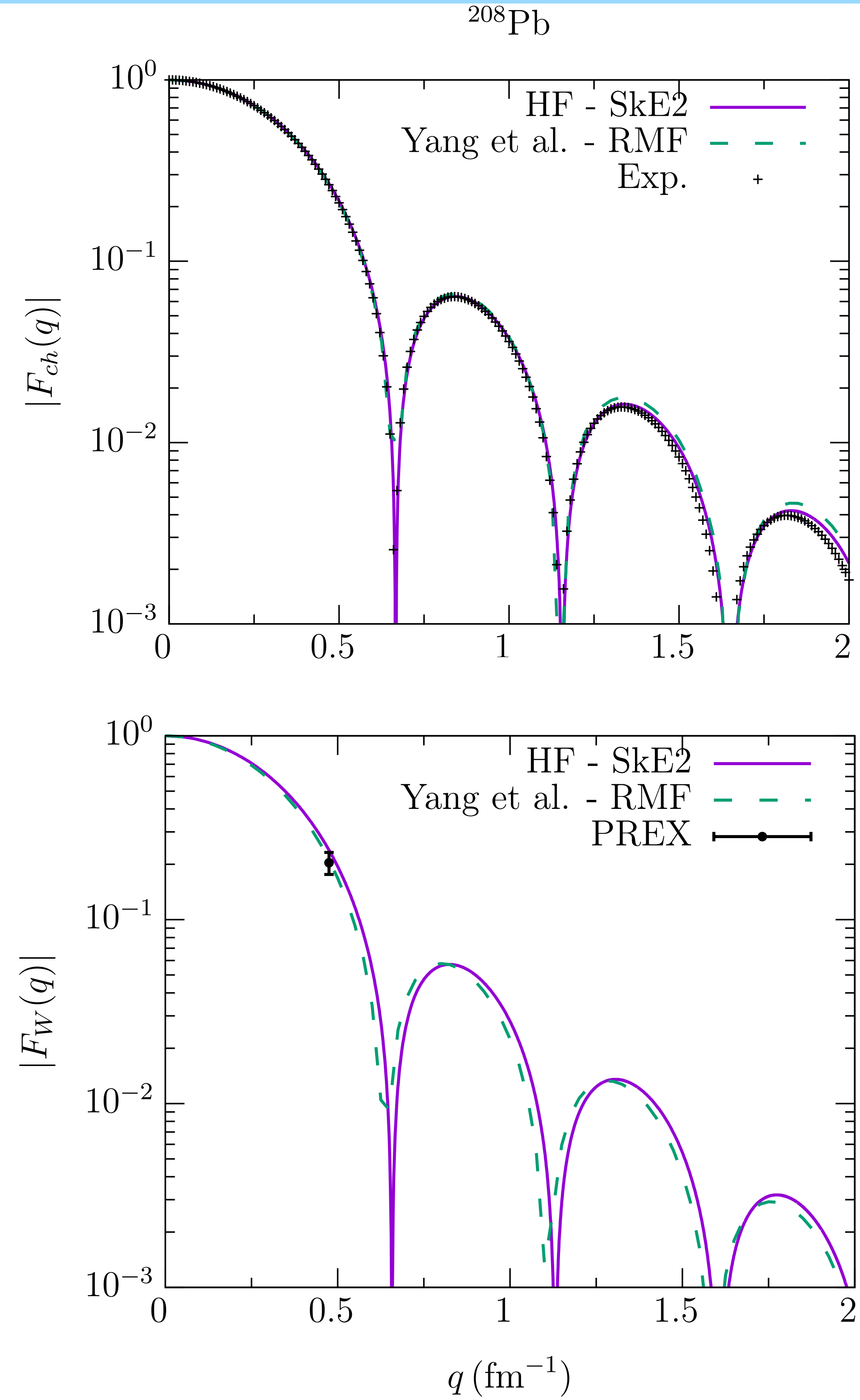

Outline

- Stopped pion sources and CEvNS
- CEvNS formalism: cross section and form factors
- Nuclear model: HF-SkE2
- **Constraining ^{40}Ar**
  - **Weak form factor and CEvNS cross section**
  - **Inelastic cross section**

COHERENT

750kg LAr detector at SNS at ORNL

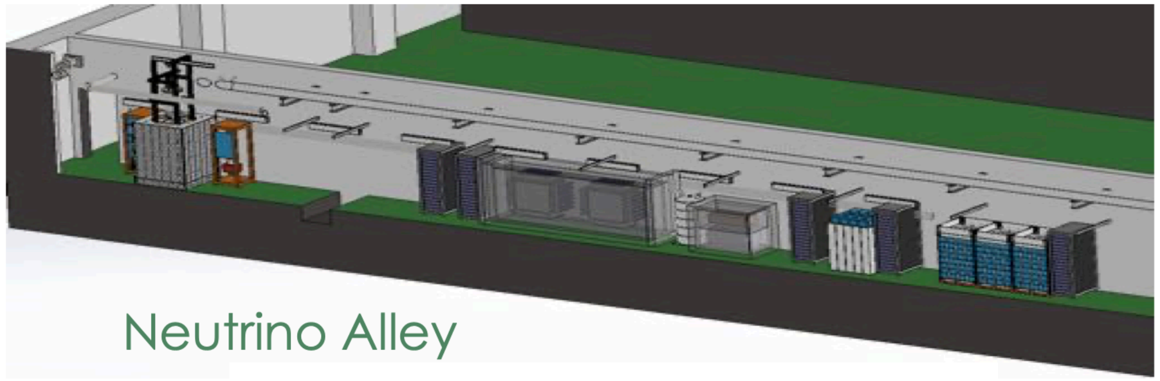

High Statistics CEvNS

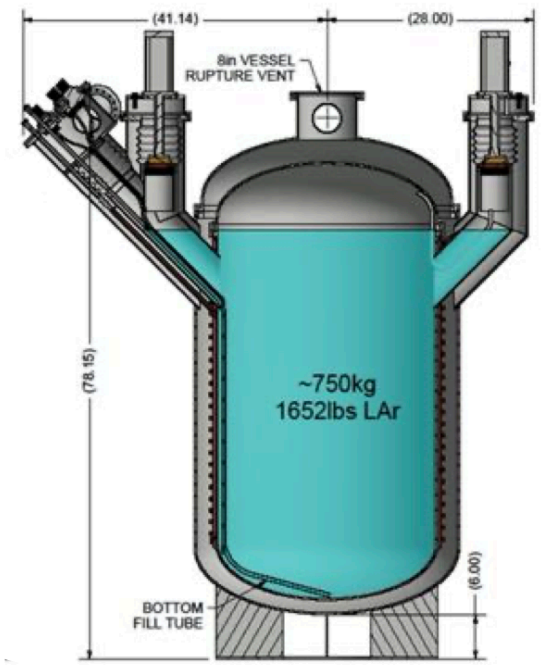

Walt Fox, IU

- 750kg LAr
- Single phase
- Light Collection Options
  - 3” PMT TPB
  - SiPM, Xenon Doping, …
- ~3000 CEvNS/yr

Jason Newby, Neutrino 2020

Coherent CAPTAIN-Mills (CCM)

10 ton LAr detector at Lujan center at LANL

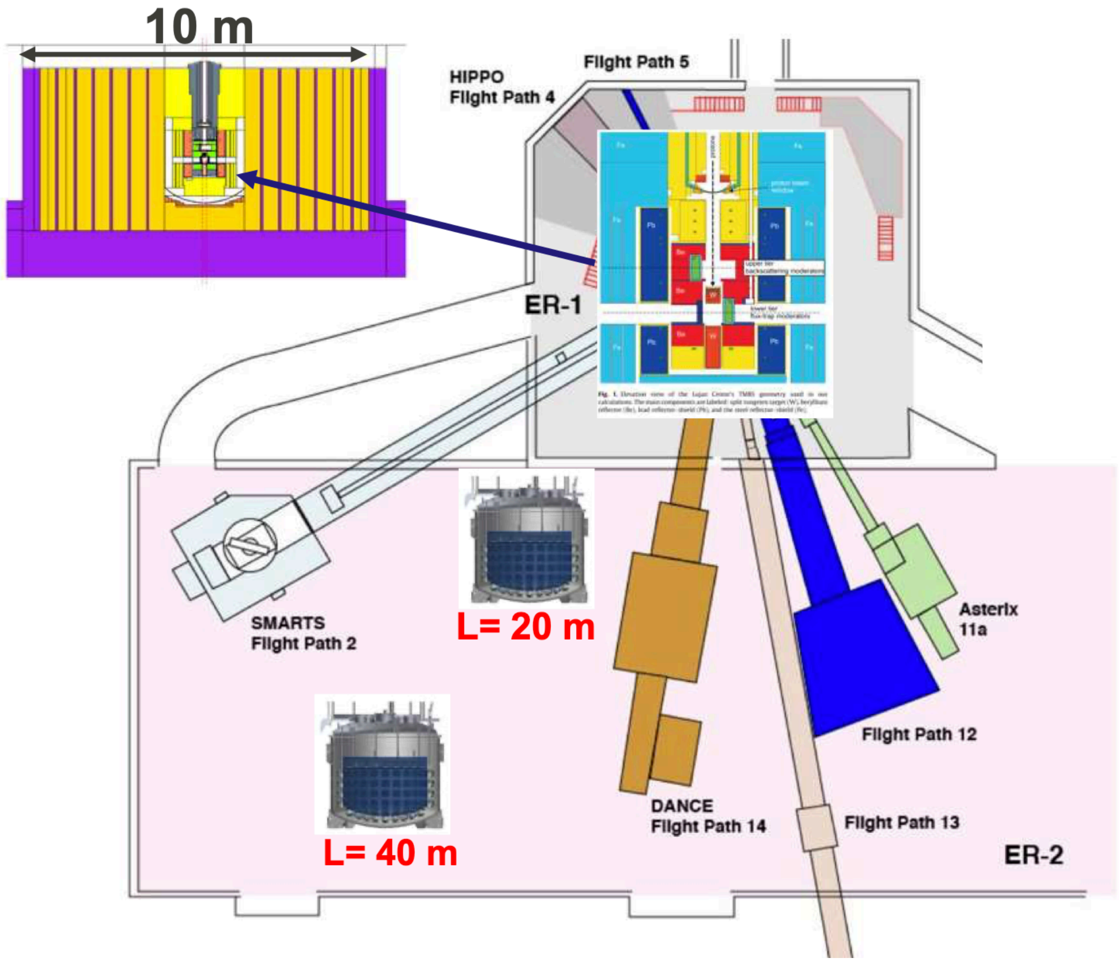

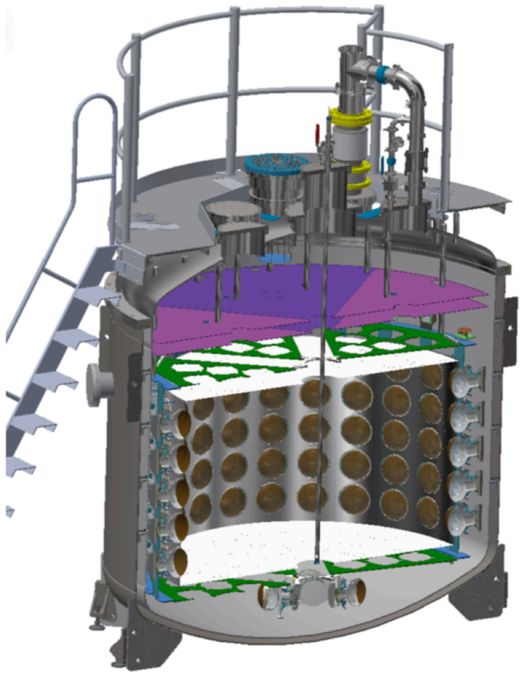

- **Charge Form Factor**

  - The ^{40}Ar charge form factor predictions describe experimental elastic electron scattering data well for $q < 2\ \mathrm{fm}^{-1}$.

  - For energies relevant for pion decay–at–rest neutrinos, the region above $q = 0.5\ \mathrm{fm}^{-1}$ does not contribute to CEvNS cross section.

Experimental data from:
C. R. Ottermann et al., Nucl. Phys. A 379, 396 (1982).

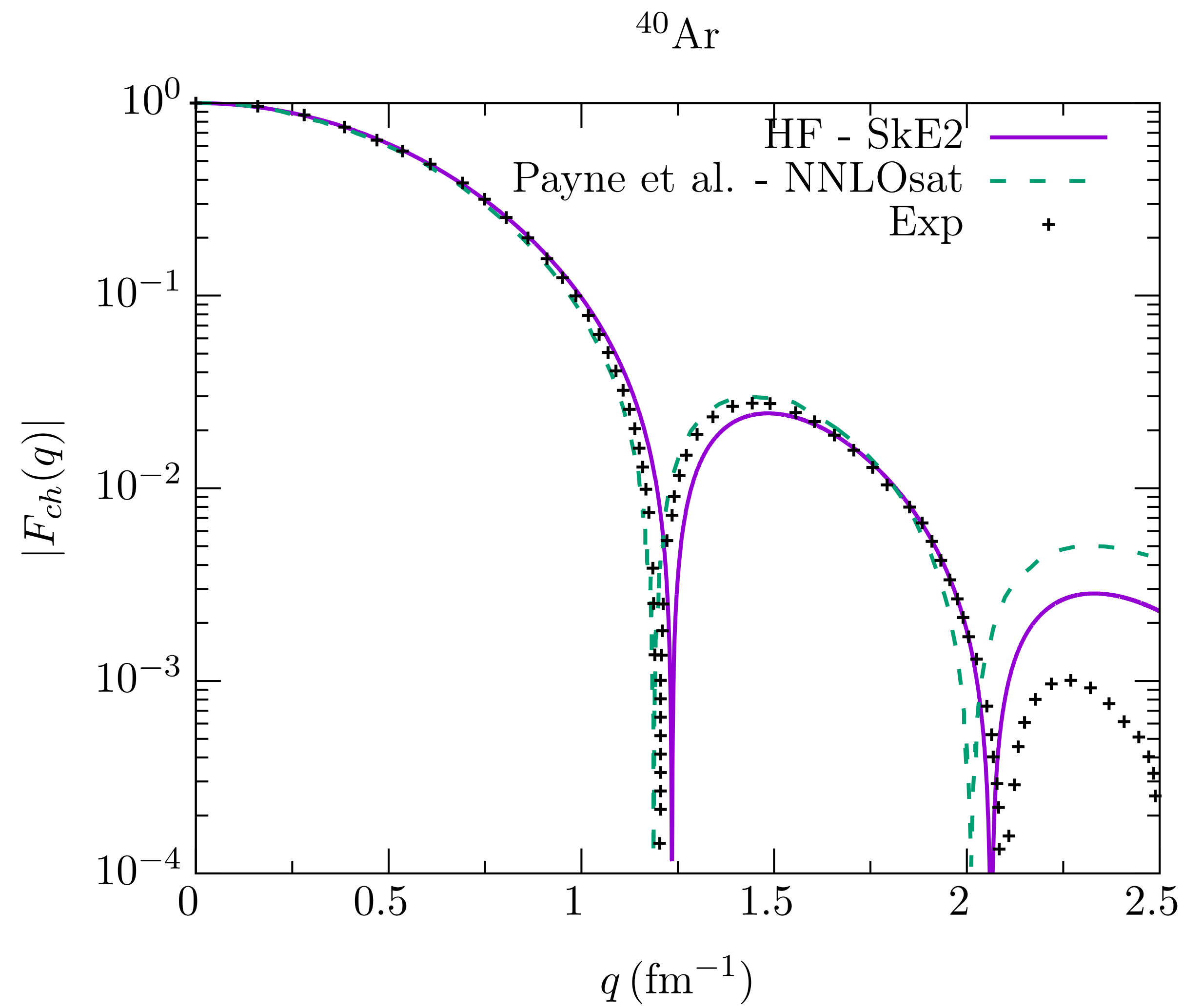

Constraining ^{40}Ar form factor and CEvNS cross section

- With no experimental data to constrain neutron distributions and weak nuclear form factors. We will try to asses a theoretical uncertainty on ^{40}Ar weak form factor and ^{40}Ar CEvNS cross section by comparing **Six** theory predictions.

A. Four microscopic many-body nuclear theory approaches that describe an accurate picture of the nuclear ground state and nucleon densities.

- The HF–SkE2 model [this work arXiv:2007.03658 [nucl-th]]
- …
- …
- …

B. Two phenomenological approaches where density distributions are represented by analytical expressions, widely used in the CEvNS community.

One can assume: $\rho_n(r) \approx \rho_p(r)$ and hence $F_n(q) \approx F_p(q) \approx F_A(q)$

- The Helm approach
- The Klein–Nystrand (KN) approach (adapted by the COHERENT collaboration)

Constraining ^{40}Ar form factor and CEvNS cross section

- With no experimental data to constrain neutron distributions and weak nuclear form factors. We will try to asses a theoretical uncertainty on ^{40}Ar weak form factor and ^{40}Ar CEvNS cross section by comparing **Six** theory predictions.

A. **Four microscopic many-body nuclear theory** approaches that describe an accurate picture of the nuclear ground state and nucleon densities.

- The HF–SkE2 model [this work arXiv:2007.03658 [nucl-th]]
- Model of Payne *et al.* [Phys. Rev. C 100, 061304 (2019)] where form factors are calculated within a coupled-cluster theory from first principles using a chiral $\mathrm{NNLO_{sat}}$ interaction.
- Model of Yang *et al.* [Phys. Rev. C 100, 054301 (2019)] where form factors are predicted within a relativistic mean–field model informed by the properties of finite nuclei and neutron stars.
- Model of Hoferichter *et al.* [arXiv:2007.08529 [hep-ph]] where form factors are calculated within a large-scale nuclear shell model.

B. **Two phenomenological approaches** where density distributions are represented by analytical expressions, widely used in the CEvNS community.

One can assume: $\rho_n(r) \approx \rho_p(r)$ and hence $F_n(q) \approx F_p(q) \approx F_A(q)$

- The Helm approach:

$$F_{\mathrm{Helm}}(q^2) = \frac{3j_1(qR_0)}{qR_0} e^{-q^2 s^2/2}$$

- The Klein–Nystrand (KN) approach (adapted by the COHERENT collaboration)

$$F_{\mathrm{KN}}(q^2) = \frac{3j_1(qR_A)}{qR_A} \left[\frac{1}{1+q^2 a_k^2}\right]$$

Weak Form Factor

- Comparison of ^{40}Ar form factor predictions from five different approaches.
- Different approaches are based on different representations of the nuclear densities.
- Let's come back to these differences in a moment.

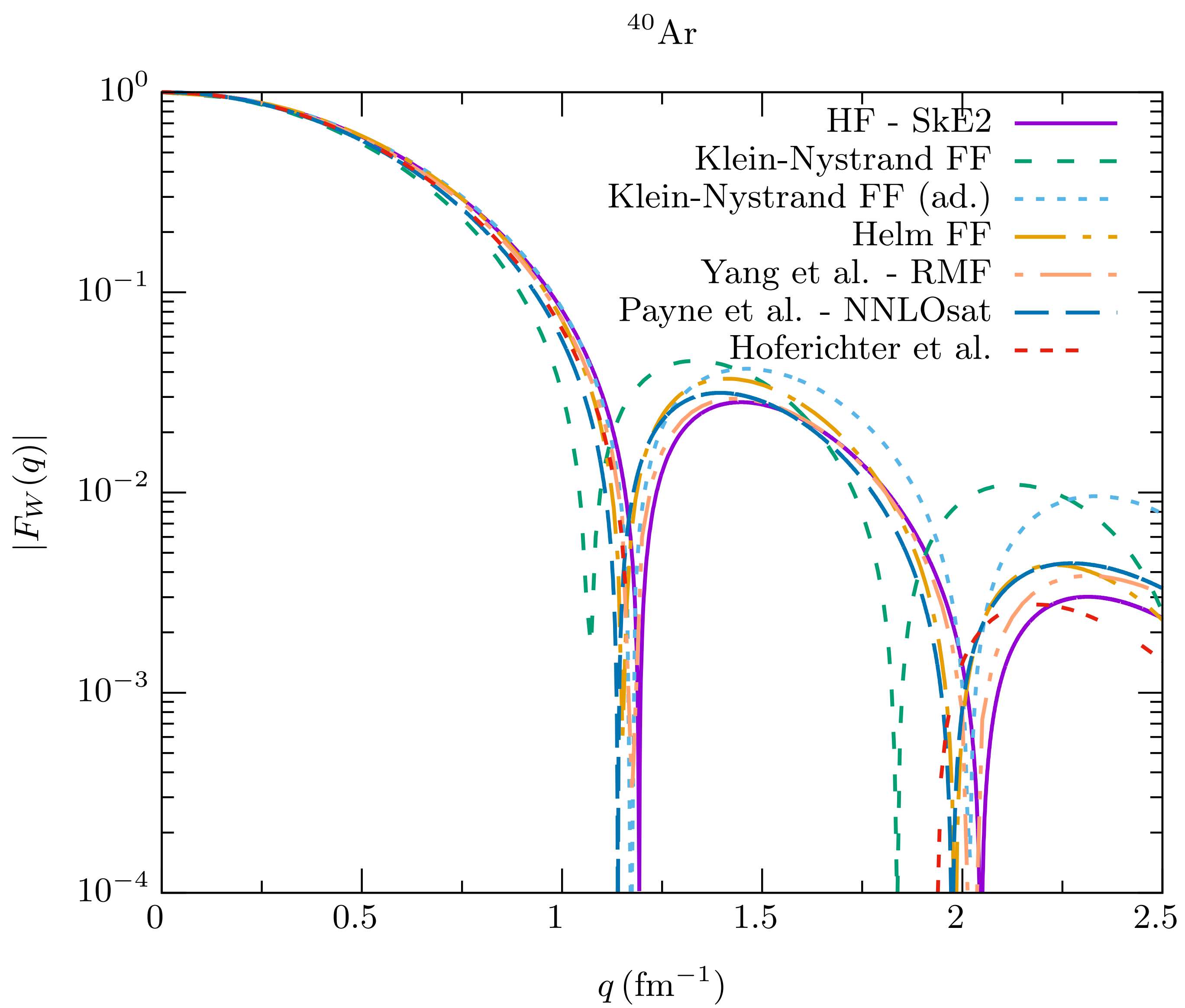

■ CEvNS cross section

- To appreciate which values of momentum transfer q are involved at different neutrino energies, we plot cumulative cross sections for ^{40}Ar at two neutrino energies.

- This is defined as the total cross section strength, integrated up to a cutoff value in the momentum transfer:

$$\sigma(q_{cutoff}) = \int_0^{q_{cutoff}} \frac{d\sigma(q)}{dq}.dq$$

- The range of cutoff values also coincides with all kinematically available momentum transfers.

- At E = 30 MeV, ^{40}Ar is only probed up to q ≈ 0.3 fm^{-1}.

- At E = 50 MeV, ^{40}Ar is only probed up to q ≈ 0.5 fm^{-1}.

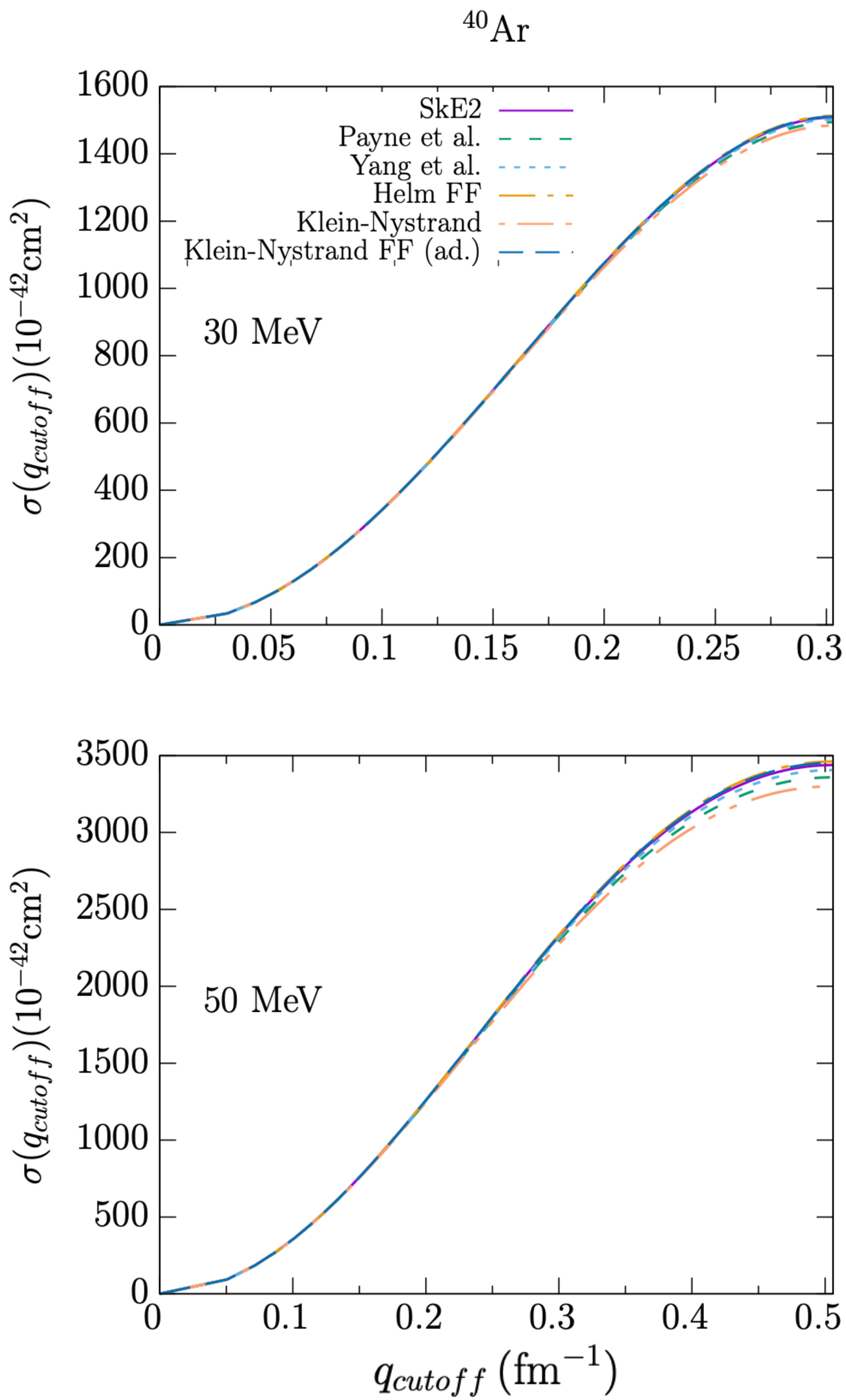

Constraining ^{40}Ar form factor and CEvNS cross section

- To quantify differences between different ^{40}Ar form factors and ^{40}Ar CEvNS cross section due to different underlying nuclear structure details. We consider quantities that emphasize the relative differences between the results of different calculations, arbitrarily using HF–SkE2 as a reference calculation, as follows:

$$\boxed{|\Delta F_{\mathrm{W}}^{i}(q)| = \frac{|F_{\mathrm{W}}^{i}(q) - F_{\mathrm{W}}^{\mathrm{HF}}(q)|}{|F_{\mathrm{W}}^{\mathrm{HF}}(q)|}}$$

$$\boxed{\Delta\sigma_{\mathrm{W}}^{i}(E) = \frac{|\sigma_{\mathrm{W}}^{i}(E) - \sigma_{\mathrm{W}}^{\mathrm{HF}}(E)|}{\sigma_{\mathrm{W}}^{\mathrm{HF}}(E)}}$$

Constraining ^{40}Ar form factor and CEvNS cross section

- To quantify differences between different ^{40}Ar form factors and ^{40}Ar CEvNS cross section due to different underlying nuclear structure details. We consider quantities that emphasize the relative differences between the results of different calculations, arbitrarily using HF–SkE2 as a reference calculation, as follows:

$$|\Delta F_{\mathrm{W}}^{i}(q)| = \frac{|F_{\mathrm{W}}^{i}(q) - F_{\mathrm{W}}^{\mathrm{HF}}(q)|}{|F_{\mathrm{W}}^{\mathrm{HF}}(q)|}$$

$$\Delta\sigma_{\mathrm{W}}^{i}(E) = \frac{|\sigma_{\mathrm{W}}^{i}(E) - \sigma_{\mathrm{W}}^{\mathrm{HF}}(E)|}{\sigma_{\mathrm{W}}^{\mathrm{HF}}(E)}$$

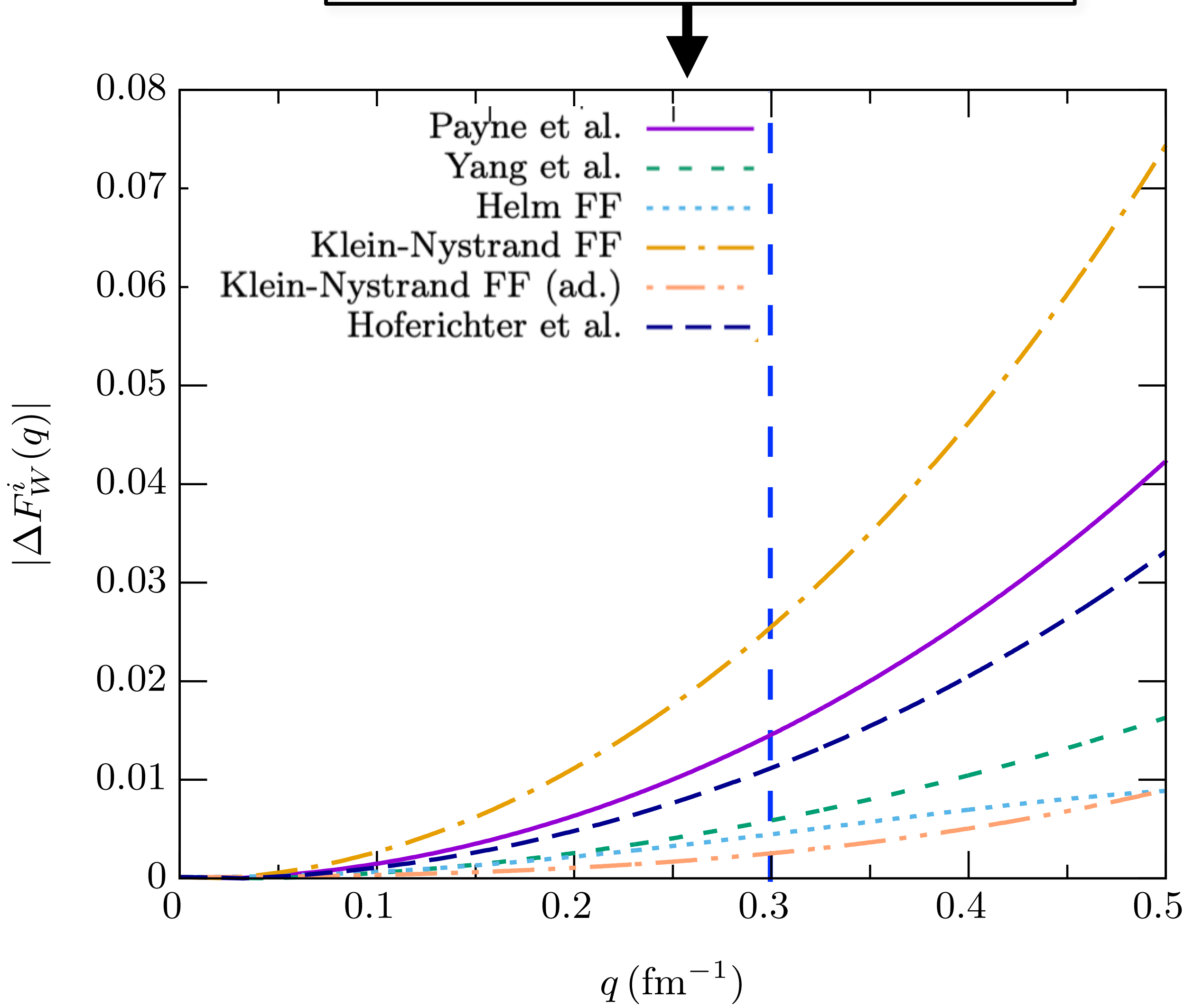

- For $q \leq 0.3$ fm^{-1} (probed by E = 30 MeV), relative differences in weak form factor predictions are < 3%.
- The differences rise rapidly at the higher end of q.
- Over the whole q $\leq$ 0.5 fm^{-1} region (probed by E $\leq$ 50 MeV), relative differences rise to $\lesssim$ 7%.

Constraining ^{40}Ar form factor and CEvNS cross section

- To quantify differences between different ^{40}Ar form factors and ^{40}Ar CEvNS cross section due to different underlying nuclear structure details. We consider quantities that emphasize the relative differences between the results of different calculations, arbitrarily using HF–SkE2 as a reference calculation, as follows:

$$|\Delta F_{\rm W}^{i}(q)| = \frac{|F_{\rm W}^{i}(q) - F_{\rm W}^{\rm HF}(q)|}{|F_{\rm W}^{\rm HF}(q)|}$$

$$\Delta\sigma_{\rm W}^{i}(E) = \frac{|\sigma_{\rm W}^{i}(E) - \sigma_{\rm W}^{\rm HF}(E)|}{\sigma_{\rm W}^{\rm HF}(E)}$$

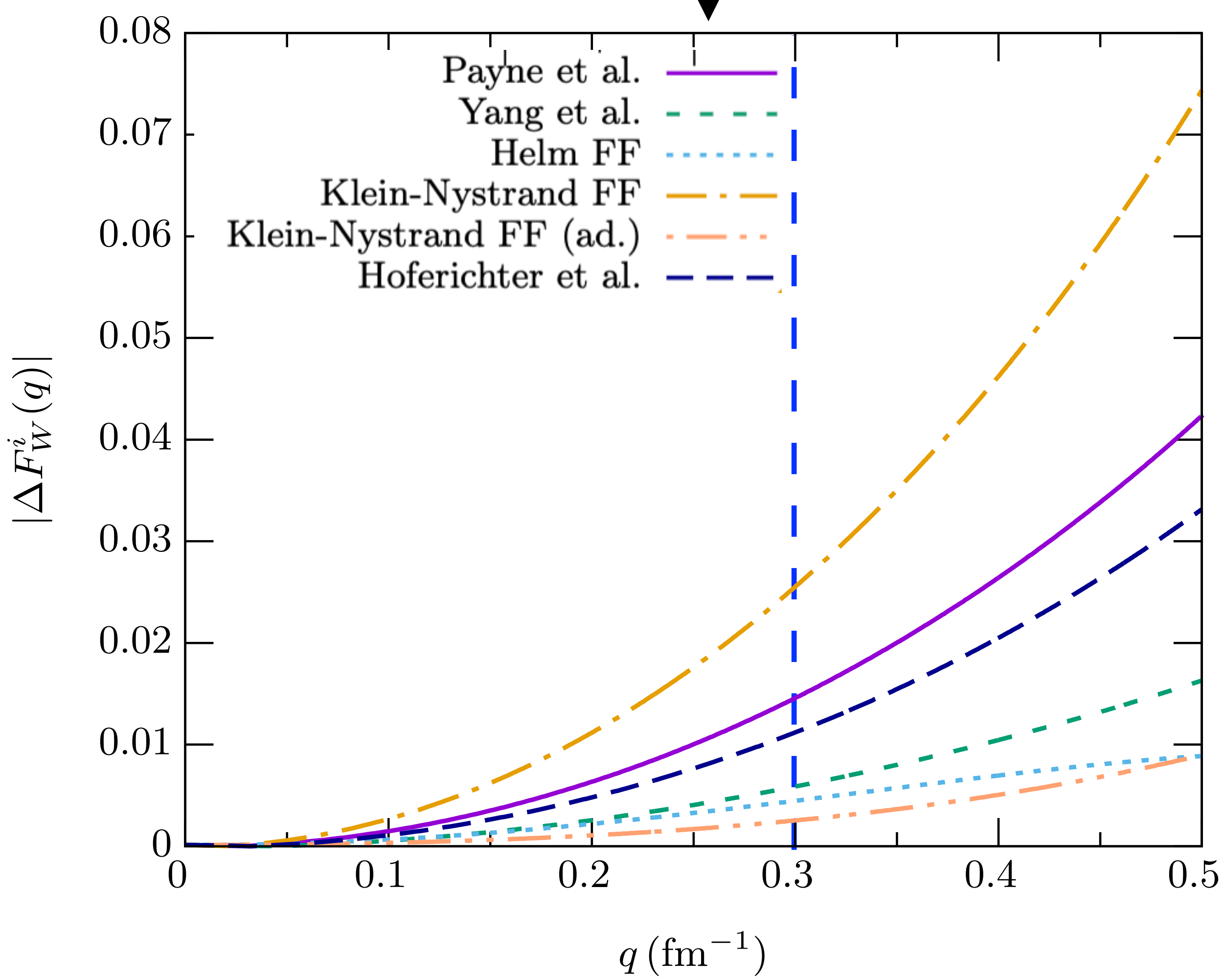

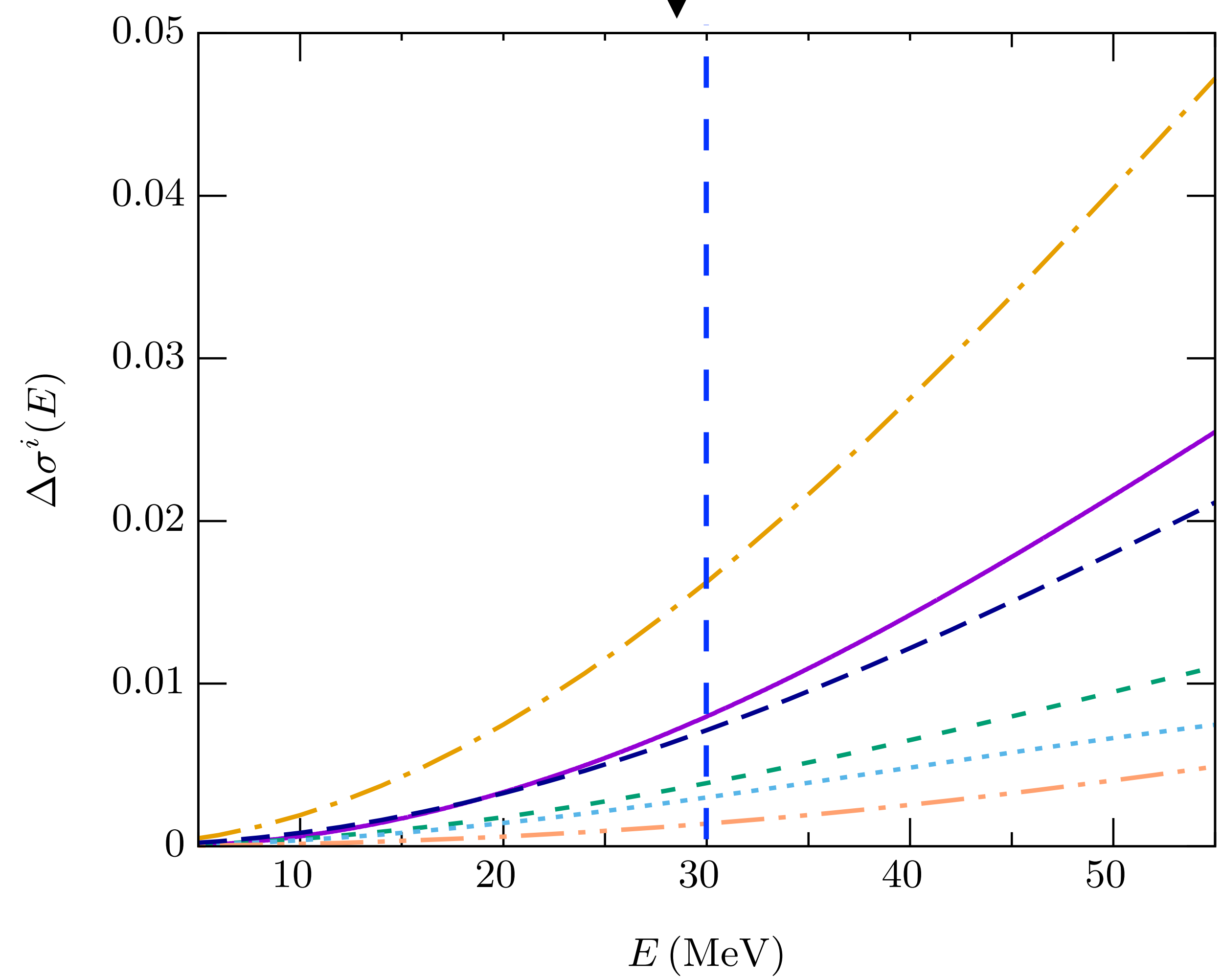

- For $q \leq 0.3$ fm^{-1} (probed by E = 30 MeV), relative differences in weak form factor predictions are < 3%.
- The differences rise rapidly at the higher end of q.
- Over the whole q $\leq$ 0.5 fm^{-1} region (probed by E $\leq$ 50 MeV), relative differences rise to $\lesssim$ 7%.

- At E = 30 MeV, the relative differences in CEvNS cross section predictions are < 2%.
- Over the whole E $\leq$ 50 MeV region, the relative differences amount to $\lesssim$ 4%.

More ^{40}Ar Results

■ **Differential cross section:**

- Differential cross section on ^{40}Ar, as a function of recoil energy T and scattering angle $\cos\theta_f$.

- Most of the cross section strength lies in the lower-end of the recoil energy and in the forward scattering as the cross section falls off rapidly at higher T (top panels) and higher θ_f values (bottom panels).

- The effects of nuclear structure physics are more prominent as the neutrino energy increases.

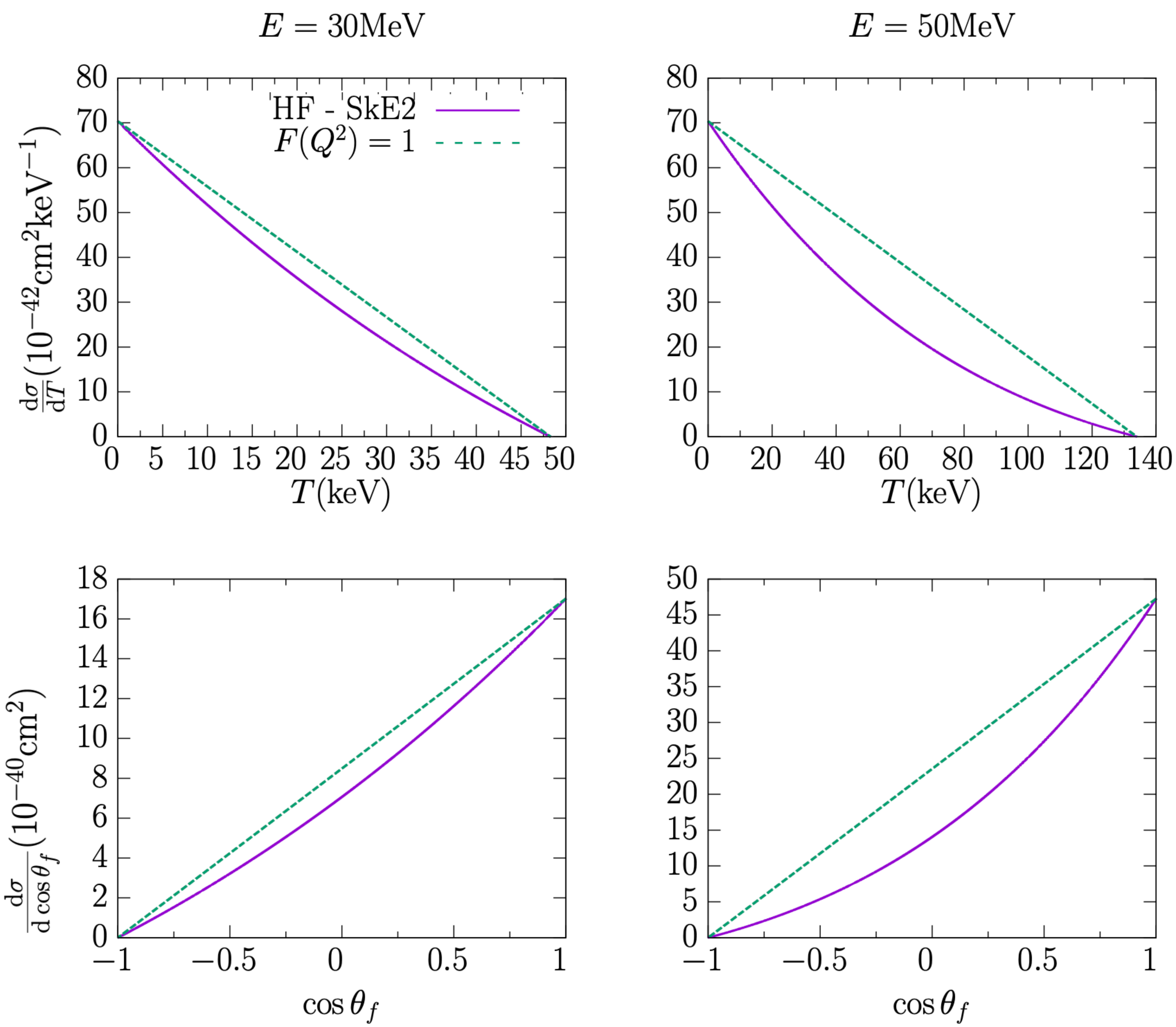

More ^{40}Ar Results

■ Comparison with COHERENT CENNS-10 data

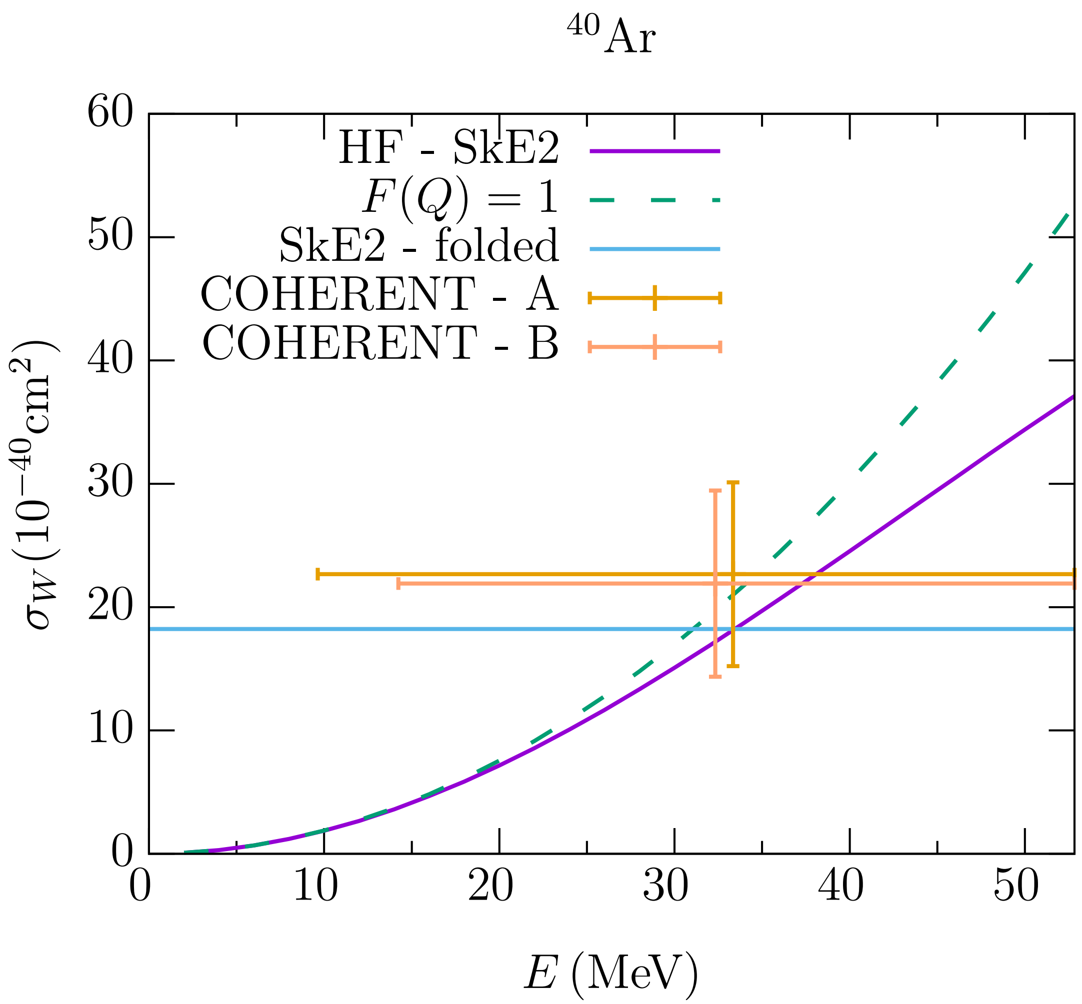

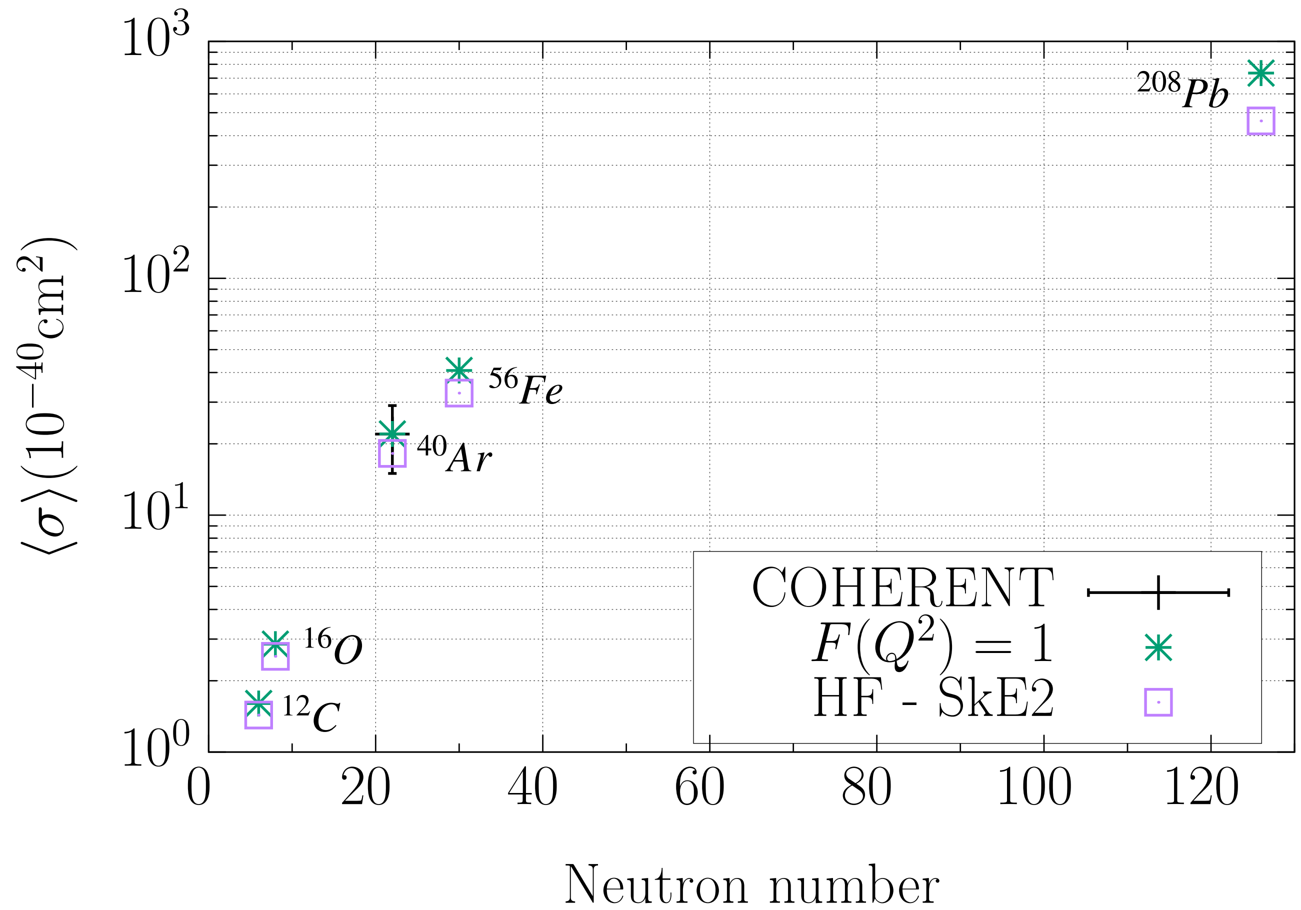

- Comparison with recent ^{40}Ar measurement performed by COHERENT collaboration. The total experimental error is dominated by statistics, amounting to ~ 30%.

^{40}Ar Inelastic Cross Section

- **HF-CRPA**

- In the quasielastic cross section calculations, the influence of long-range correlations between the nucleons is introduced through the continuum Random Phase Approximation (CRPA) on top of the HF-SkE2 approach.
- CRPA effects are vital to describe the quasielastic scattering process where the nucleus can be excited to low-lying collective nuclear states.
- The local RPA-polarization propagator is obtained by an iteration to all orders of the first order contribution to the particle-hole Green's function.

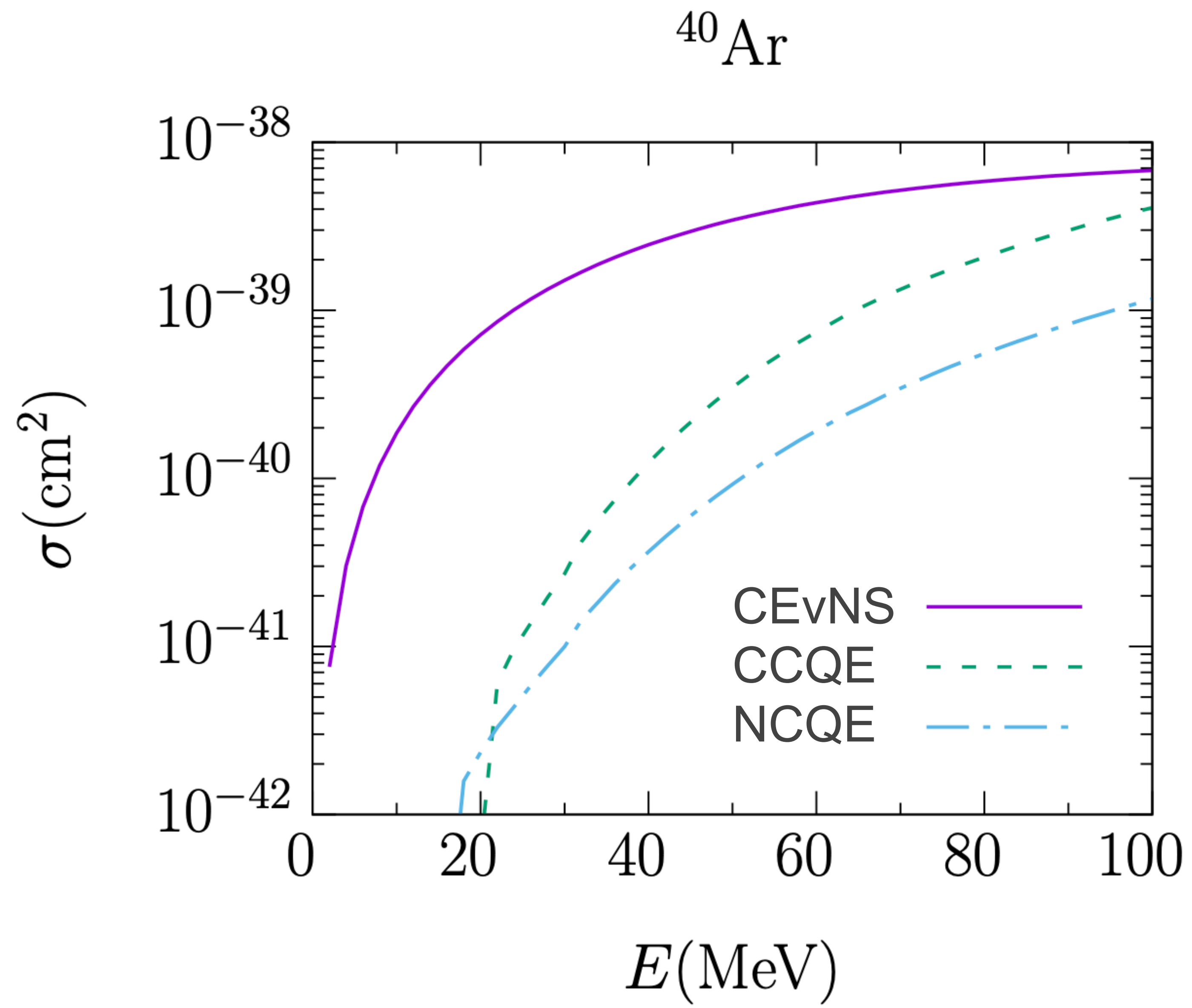

$$\Pi^{(RPA)}(x_1,x_2;E_x) = \Pi^{(0)}(x_1,x_2;E_x) + \frac{1}{\hbar}\int dx dx'\ \Pi^0(x_1,x;E_x) \times \tilde{V}(x,x')\ \Pi^{(RPA)}(x',x_2;E_x)$$

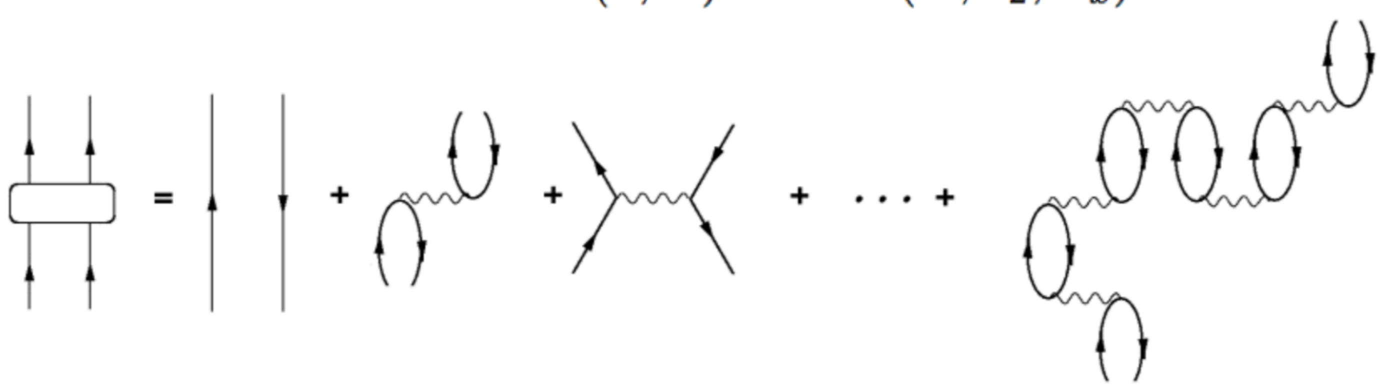

^{40}Ar Inelastic Cross Section

■ HF-CRPA

- In the quasielastic cross section calculations, the influence of long-range correlations between the nucleons is introduced through the continuum Random Phase Approximation (CRPA) on top of the HF-SkE2 approach.
- CRPA effects are vital to describe the quasielastic scattering process where the nucleus can be excited to low-lying collective nuclear states.
- The local RPA-polarization propagator is obtained by an iteration to all orders of the first order contribution to the particle-hole Green's function.

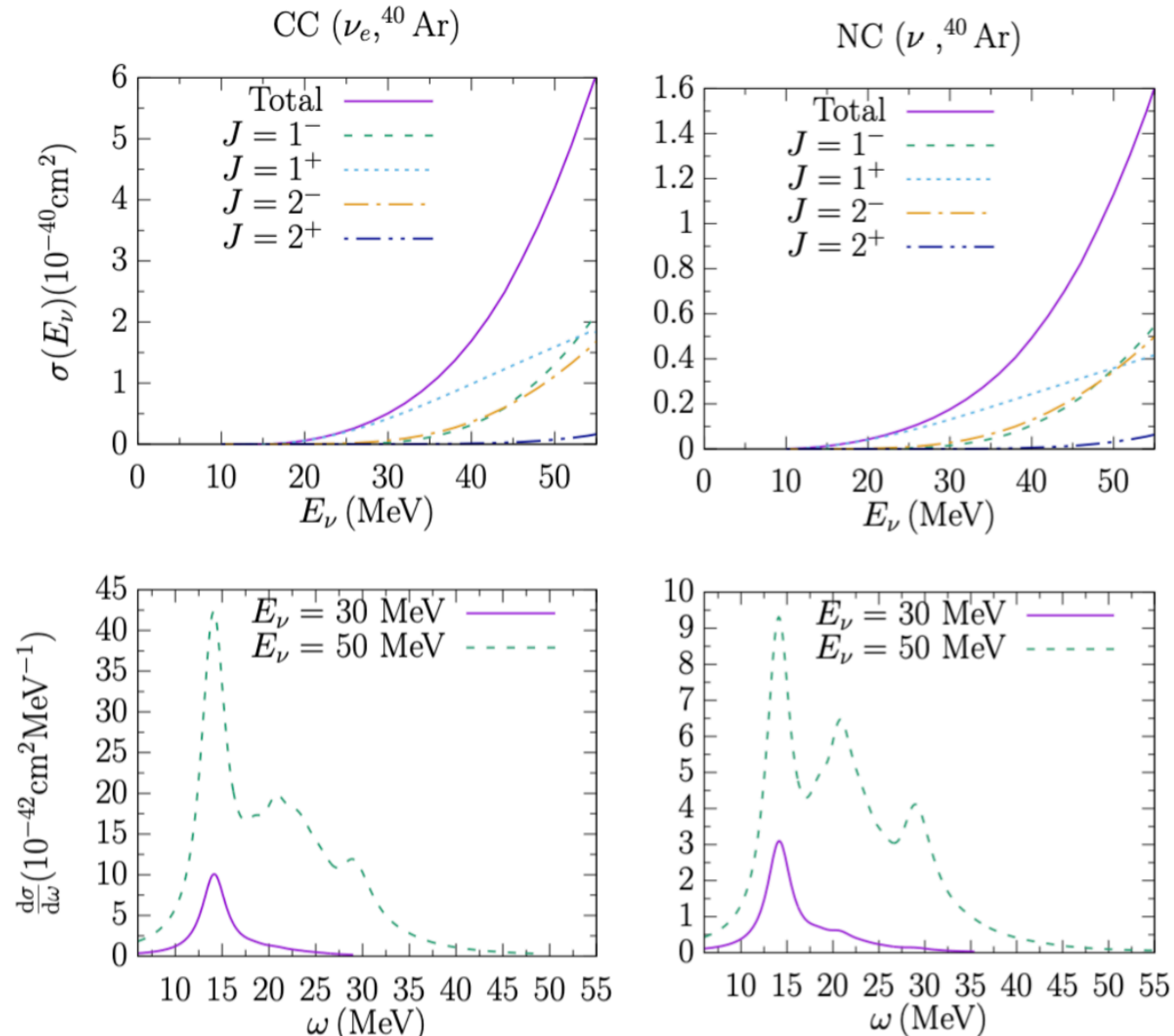

$$\Pi^{(RPA)}(x_1, x_2; E_x) = \Pi^{(0)}(x_1, x_2; E_x) + \frac{1}{\hbar}\int dx dx' \, \Pi^0(x_1, x; E_x) \times \tilde{V}(x, x') \, \Pi^{(RPA)}(x', x_2; E_x)$$

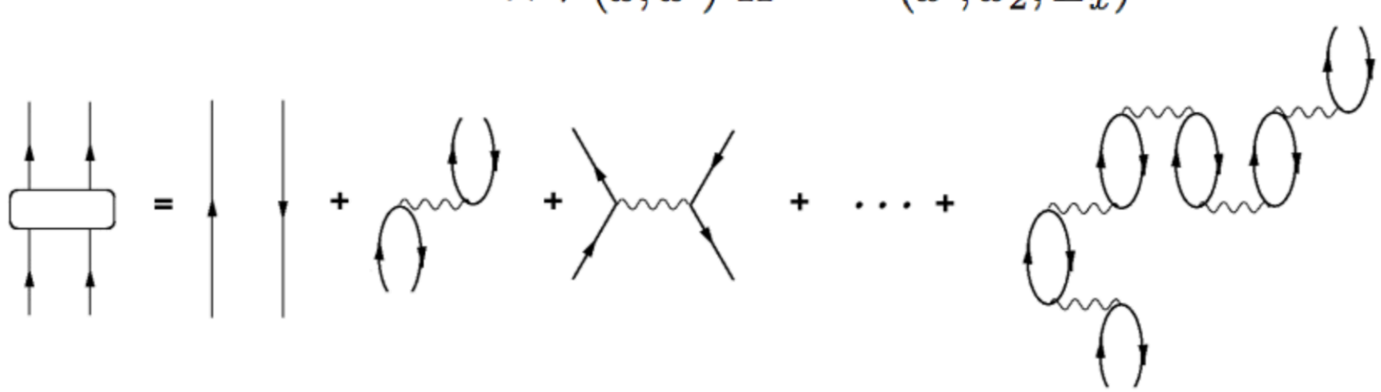

Summary

- Experimental observation of CEvNS opened a new portal of searching weakly interacting new physics at low energies. SM expectation of CEvNS cross section have to be know at a precision that allows resolving degeneracies in the standard and non-standard physics observables.

- An accurate description of the neutron density distribution and weak form factor is vital to the CEvNS program since any experimentally measured deviation from the expected CEvNS event rate can point to new physics or to unconstrained nuclear physics.

- We presented calculations of nucleon densities and form factors within a microscopic many–body nuclear theory model where the nuclear ground state is described in a Hartree–Fock (HF) approach with a Skyrme (SkE2) nuclear potential. The model describes charge form factor data remarkably well.

- We paid special attention to ^{40}Ar, and provide an assessment of theoretical uncertainty on ^{40}Ar weak form factor and ^{40}Ar CEvNS cross section by comparing different nuclear theory and phenomenological predictions.

- We present a consistent description of both coherent elastic and inelastic cross sections.